

Research article

[urn:lsid:zoobank.org:pub:400FEC6E-8E57-4207-A0F9-2AC4F5290FE8](https://zoobank.org/pub:400FEC6E-8E57-4207-A0F9-2AC4F5290FE8)

A new cryptic species of *Pithecopus* (Anura, Phyllomedusidae) in north-eastern Brazil

Felipe Silva de ANDRADE^{1,*}, Isabelle Aquemi HAGA², Johnny Sousa FERREIRA³,
Shirlei Maria RECCO-PIMENTEL⁴, Luís Felipe TOLEDO⁵ &
Daniel Pacheco BRUSCHI⁶

^{1,5}Laboratório de História Natural de Anfíbios Brasileiros (LaHNAB),
Departamento de Biologia Animal, Instituto de Biologia,
Universidade Estadual de Campinas (UNICAMP), Campinas, São Paulo, Brazil.

^{1,2}Laboratório de Taxonomia e Sistemática de Anuros Neotropicais (LTSAN),
Faculdade de Ciências Integradas do Pontal (FACIP), Universidade Federal de Uberlândia (UFU),
Ituiutaba, Minas Gerais, Brazil.

^{3,6}Programa de Pós-graduação em Genética, Departamento de Genética, Setor de Ciências Biológicas,
Universidade Federal do Paraná (UFPR), Curitiba, Paraná, Brazil.

⁴Departamento de Biologia Estrutural e Funcional, Instituto de Biologia,
Universidade Estadual de Campinas (UNICAMP), Campinas, São Paulo, Brazil.

* Corresponding author: felipe_andrade@ymail.com

²Email: hagaisabelle@gmail.com

³Email: johnny.sf@gmail.com

⁴Email: shirlei@unicamp.br

⁵Email: toledosapo@gmail.com

⁶Email: danielpachecobruschi@gmail.com

¹[urn:lsid:zoobank.org:author:A6B5147E-158C-459C-97A7-B4E7ADE3DB23](https://zoobank.org/author:A6B5147E-158C-459C-97A7-B4E7ADE3DB23)

²[urn:lsid:zoobank.org:author:10EA92D6-7C2E-4141-A912-6E45B4EDF321](https://zoobank.org/author:10EA92D6-7C2E-4141-A912-6E45B4EDF321)

³[urn:lsid:zoobank.org:author:18B76F10-1DA7-44F3-8DC5-6C602B650316](https://zoobank.org/author:18B76F10-1DA7-44F3-8DC5-6C602B650316)

⁴[urn:lsid:zoobank.org:author:4F71D5BF-7DCD-4DF7-B96A-EAE1A757EF8D](https://zoobank.org/author:4F71D5BF-7DCD-4DF7-B96A-EAE1A757EF8D)

⁵[urn:lsid:zoobank.org:author:2430A30A-DB39-4C75-9508-F9489557A223](https://zoobank.org/author:2430A30A-DB39-4C75-9508-F9489557A223)

⁶[urn:lsid:zoobank.org:author:A989E6C1-D040-4F00-AB15-C6CED003DC5E](https://zoobank.org/author:A989E6C1-D040-4F00-AB15-C6CED003DC5E)

Abstract. The genus of Neotropical frogs *Pithecopus* includes 11 species occurring east of the Andes from southern Venezuela to northern Argentina. Recent genetic approaches pointed out an unusual genetic diversity among populations from localities in north-eastern Brazil recognized as *P. nordestinus*. In fact, one of these studies confirmed the hypothesis that the São Francisco River acted as an effective geographical barrier during vicariant events in the evolutionary history of *P. nordestinus*, resulting in two principal, highly divergent clades. Herein we formally describe this divergent clade as a new cryptic species of *Pithecopus* from north-eastern Brazil, the sister clade of *P. nordestinus*. It differs from other species of *Pithecopus*, except for *P. azureus* and *P. nordestinus*, by its small body size, lack of the reticulate pattern on flanks, smaller head width, and advertisement calls generally composed of a three-pulsed core.

Keywords. Integrative taxonomy, *Pithecopus nordestinus*, São Francisco River, phenotypically cryptic species.

Andrade F.S., Haga I.A., Ferreira J.S., Recco-Pimentel S.M., Toledo L.F. & Bruschi D.P. 2020. A new cryptic species of *Pithecopus* (Anura, Phyllomedusidae) in north-eastern Brazil. *European Journal of Taxonomy* 723: 108–134. <https://doi.org/10.5852/ejt.2020.723.1147>

Introduction

The genus *Pithecopus* Cope, 1866 comprises 11 tropical South American species occurring east of the Andes from southern Venezuela to northern Argentina (Faivovich *et al.* 2010; Duellman *et al.* 2016; Frost 2020). Phylogenetic inferences for species of *Pithecopus* recovered two well-supported clades with strong biogeographical cohesiveness (Faivovich *et al.* 2010; Duellman *et al.* 2016). One of them is the highland clade composed of *P. ayeaye* Lutz, 1966, *P. megacephalus* (Miranda-Ribeiro, 1926), *P. centralis* (Bokermann, 1965), *P. oreades* (Brandão, 2002) and *P. rusticus* (Bruschi, Lucas, Garcia & Recco-Pimentel, 2015). The other one is the lowland clade that comprises the species *Pithecopus palliatus* (Peters, 1873), *P. azureus* (Cope, 1862), *P. hypochondrialis* (Daudin, 1800), *P. araguaius* Haga, Andrade, Bruschi, Recco-Pimentel & Giaretta, 2017 and *P. nordestinus* (Caramaschi, 2006) (Faivovich *et al.* 2010). The species of the lowland clade have large overlaps in their acoustic and morphological traits, hence complex species delimitations (mainly among *P. azureus*, *P. nordestinus*, *P. hypochondrialis* and *P. araguaius*) (Haga *et al.* 2017a, 2017b).

Pithecopus nordestinus is a charismatic treefrog widely distributed in the Atlantic Forest and adjacent areas of Caatinga scrublands in north-eastern Brazil, with records of occurrence in the states of Maranhão, Piauí, Ceará, Rio Grande do Norte, Paraíba, Pernambuco, Alagoas, Sergipe, Bahia and Minas Gerais (Frost 2020). Faivovich *et al.* (2010) reported unusual genetic diversity among populations recognized as *P. nordestinus* collected in three distinct localities in north-eastern Brazil. Estimations of genetic distances among mitochondrial cytochrome b sequences reported conspicuous variation range among the three collection sites (10.4–16.7%) (Faivovich *et al.* 2010). Extensive sampling and phylogenetic inferences based on multilocus DNA sequences detected deep and ancient phylogeographic breaks between populations currently assigned to *P. nordestinus* from opposite margins of the São Francisco River (SFR), potentially due to historical shifts in the course of this geographical barrier, deciphering the source of this genetic divergence (Bruschi *et al.* 2019).

Confronted by recent molecular evidence indicating the existence of two lineages within this taxon (Bruschi *et al.* 2019), the question was to ascertain if these two monophyletic lineages of *P. nordestinus* represented two distinct species? This question was hitherto unanswered, due to the lack of an integrative approach that would evaluate evidence from different sources, including morphological and acoustic traits. Herein, we provide a solution to this taxonomic problem, which could be fundamental to better comprehension and management of regional biodiversity (Fišer *et al.* 2018). We investigated genotypic and phenotypic (morphological and acoustics) evidence to assess the taxonomical status of the populations assigned to *P. nordestinus*. Our results indicate the existence of a new phenotypically cryptic species of *Pithecopus* from north-eastern Brazil, which we describe in the present study.

Material and methods

Specimens collected

Specimens were collected under authorisation number #17242-3 issued by SISBIO/Instituto Chico Mendes de Conservação da Biodiversidade. We killed the specimens using anaesthetic (5% Lidocaine) application on the skin, according to recommendations of the Herpetological Animal Care and Use

Committee (HACC) of the American Society of Ichthyologists and Herpetologists (available at https://asih.org/sites/default/files/2018-05/guidelines_herps_research_2004.pdf), and approved by SISBIO/Institute Chico Mendes de Conservação da Biodiversidade. Type specimens were deposited in the amphibian collection of Museu de Zoologia “prof. Dr. Adão José Cardoso” (ZUEC) of the Universidade Estadual de Campinas (UNICAMP), Campinas, São Paulo, Brazil.

Taxa and specimens examined

Twenty-eight individuals (24 adult males and four adult females) of the new species were collected in the municipality of Limoeiro (7°52'29.0" S, 35°27'01.1" W; 150 m a.s.l.; datum = WGS84), state of Pernambuco (PE), Brazil. We also collected and examined 150 additional specimens of the new species (135 adult males and 15 adult females) from 16 other localities in four Brazilian states (Fig. 1). We examined and measured the following types: holotype (MNRJ 13607) and paratypes (MNRJ 13602–6, 13608–11, 13598–600, 35223 to 35228, 60097) of *P. nordestinus*, and holotype (AAG-UFU 3444) and paratypes (AAG-UFU 3442–3, 3445–9, 4877–82, ZUEC 21657–60) of *P. araguauius*. Types and additional specimens of all analysed species are deposited in:

- AAG-UFU = Collection of frogs of the Museu de Biodiversidade do Cerrado, Universidade Federal de Uberlândia (UFU), Uberlândia, Minas Gerais, Brazil
CFBH = Célio F.B. Haddad amphibian collection, Universidade Estadual Paulista (Unesp), Rio Claro, State of São Paulo, Brazil
MNRJ = Museu Nacional, Universidade Federal do Rio de Janeiro (UFRJ), Rio de Janeiro, State of Rio de Janeiro, Brazil
ZUEC = Museu de Zoologia “prof. Dr. Adão José Cardoso” of the Universidade Estadual de Campinas (UNICAMP), Campinas, São Paulo, Brazil

Additionally, we examined specimens of *P. palliatus*, *P. rohdei* (Mertens, 1926), *P. ayeaye*, *P. megacephalus*, *P. centralis*, *P. oreades* and *P. rusticus*. The complete list of specimens examined is available in the Appendix.

Morphometry

Adult individuals were measured using a Mitutoyo Absolute digital calliper CD-6” CSX to the nearest 0.1 mm. Twelve morphometric traits were measured following Watters *et al.* (2016): snout-vent length (SVL), hand length (HAL), forearm length (FAL), upper arm length (UAL), thigh length (THL), foot length (FL), head length (HL), head width (HW), eye diameter (ED), internarial distance (IND), tibia length (TL) (=shank length), tarsus length (TAL), tympanum diameter (TD) and eye-nostril distance (END). The axilla-groin length (AGL) was measured according to Clemente-Carvalho *et al.* (2012). The shape of the snout in dorsal and lateral view follows Duellman (1970).

For comparisons with the most closely related species (the lowland species of *Pithecopus*), we used the same dataset recently used to describe *P. araguauius* (Haga *et al.* 2017a): 21 types (holotype + 20 paratopotypes) and 31 non-type specimens of *P. nordestinus* from Alagoinhas (Bahia), Areia Branca (Sergipe) and Laranjeiras (Sergipe); 18 types (holotype + 17 paratopotypes) and 18 non-type specimens of *P. araguauius* from Chapada dos Guimarães (Mato Grosso) and Santa Terezinha (Mato Grosso); 13 topotypes from Asunción, Paraguay, one non-type specimen from Corrientes, Argentina, and 11 non-type specimens from Bela Vista (Mato Grosso do Sul) (the nearest acoustic sample from its type-locality) of *P. azureus*. Further details on examined specimens are in the Appendix.

Bioacoustics

Seventy-three advertisement calls of six males of the new species were recorded between 19:11 and 22:07 on four field trips in May 2011 (days 7, 17, 22 and 24; temperature of air 28–29°C and water

25–26°C). Recordings were obtained with a Marantz PMD 222 cassette recorder, coupled to an Audio-Technica AT835b directional microphone. Recordings were digitised at 48 kHz and 24 bit resolution.

For acoustic comparisons, we also used the dataset of Haga *et al.* (2017a), supplemented with three recordings of *P. nordestinus* (FNJV 31155, FNJV 45456, FNJV 45468) that were deposited in the Fonoteca Neotropical Jacques Viellard (FNJV). Therefore, the complete comparative dataset includes advertisement calls from four males of *P. azureus* (Haga *et al.* 2017b); 105 calls from six males of *P. nordestinus* (from the municipalities of Areia Branca, Itabaiana and Maruim, Sergipe; Gandu and Igrapiúna, Bahia); 24 calls from seven males of the type-series of *P. araguaius*; 212 calls of 41 males of

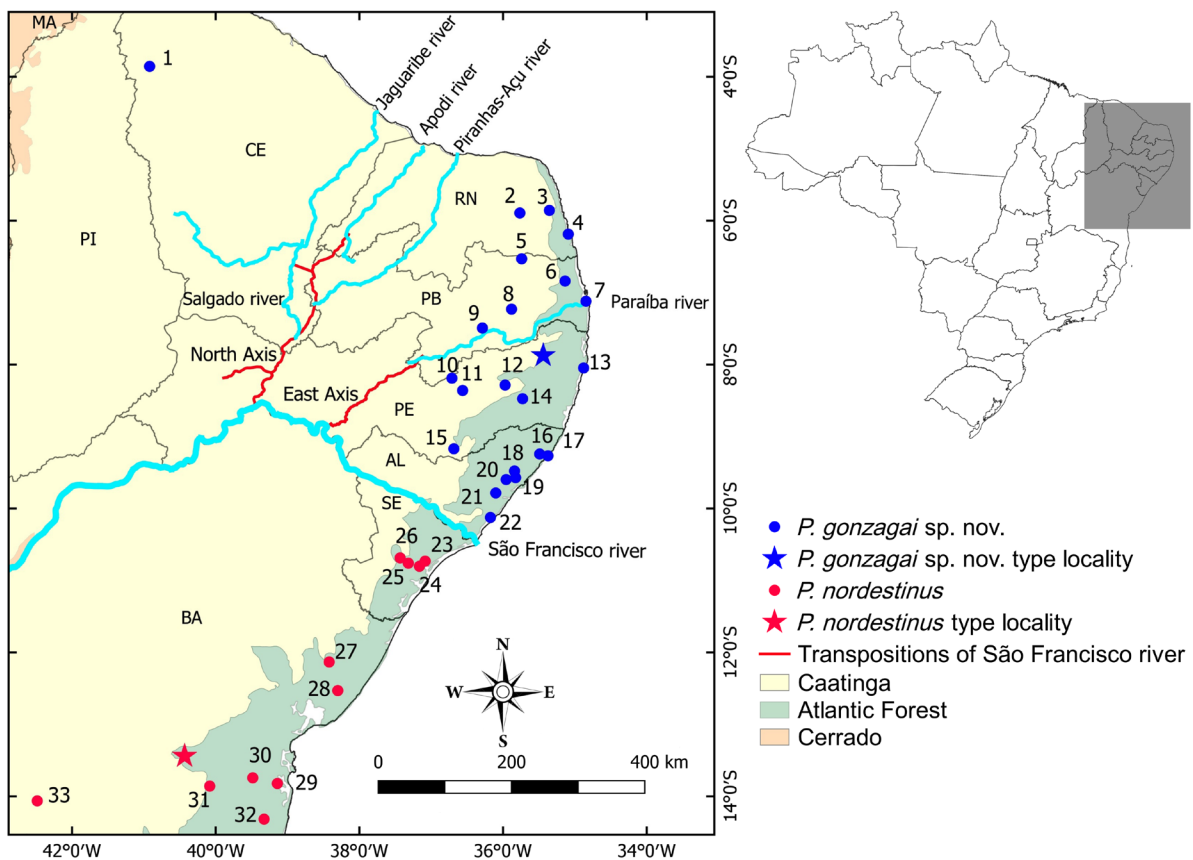


Fig. 1. Map showing molecular, morphological and acoustic samples used in the comparisons between *Pithecopus gonzagai* sp. nov. (red dots and star) and *P. nordestinus* (Caramaschi, 2006) (blue dots and star) in north-eastern Brazil. We indicate the original São Francisco River path (blue) and the new path after the installation of the North and East Axes (in red) as a result of the Transposition Project. Municipalities: 1 = Ubajara (CE); 2 = São Paulo do Potengi (RN); 3 = Macaíba (RN); 4 = Tibau do Sul (RN); 5 = Araruna (PB); 6 = Mamanguape (PB); 7 = João Pessoa (PB); 8 = Campina Grande (PB); 9 = Cabaceiras (PB); 10 = Poção (PE); 11 = Sanharó (PE); 12 = Caruaru (PE); 13 = Recife (PE); 14 = Bonito (PE); 15 = Bom Conselho (PE); 16 = Passos do Camaragibe (AL); 17 = São Miguel dos Milagres (AL); 18 = Rio Largo (AL); 19 = Satuba (AL); 20 = Pilar (AL); 21 = São Miguel dos Campos (AL); 22 = Coruripe (AL); 23 = Maruim (SE); 24 = Laranjeiras (SE); 25 = Areia Branca (SE); 26 = Itabaiana (SE); 27 = Alagoinhas (BA); 28 = Mata de São João (BA); 29 = Igrapiúna (BA); 30 = Gandu (BA); 31 = Jequié (BA); 32 = Aurelino Leal (BA); 33 = Caetité (BA); red star = type locality of *P. gonzagai* sp. nov.: Limoeiro (PE); blue star = type locality of *P. nordestinus*: Maracás (BA). Brazilian states: AL = Alagoas; BA = Bahia; CE = Ceará; PB = Paraíba; PE = Pernambuco; RN = Rio Grande do Norte; SE = Sergipe.

P. hypochondrialis (from the municipalities of Serra do Navio, Amapá; Barra do Garças, Mato Grosso; Brasília, Distrito Federal; Araguari and Uberlândia, Minas Gerais; Padre Bernardo, Pirenópolis and Uruaçu, Goiás). Call vouchers are listed in [Supplementary file 1](#). We reanalysed two males and 34 calls of *P. nordestinus* (FNJV 45456, FNJV 45468) that were used in Vilaça *et al.* (2011). As different authors may analyze calls differently and in order to ensure the reliability of our results, we have based the acoustic comparisons only on our own data.

Sound files are deposited in the Arquivo Sonoro da Coleção de Anuros, UFU, and FNJV, UNICAMP. Call descriptions and the acoustic terminology follow Köhler *et al.* (2017) and Haga *et al.* (2017a: appendix B – S1 table: Acoustic terminology employed for the species of *Pithecopus*). According to Haga *et al.* (2017a), the calls of some species of *Pithecopus* often have a few low-amplitude isolated pulses at the end (more common) or at the beginning (unusual). We used the main (high-amplitude) group of pulses of each call (hereafter called ‘core portion’) of the new species, *P. araguaius*, *P. hypochondrialis*, *P. azureus* and *P. nordestinus* to compare call traits equivalently among these species. Analysed sound files are listed in [Supplementary file 1](#).

We calculated means and standard deviations (SD) for each individual and then the overall mean and SD was calculated based on those values, whereas the range encompassed the minimum and maximum values for the whole sample. We analysed calls using Raven Pro 1.5, 64 bit version (Bioacoustics Research Program 2014) with the following settings: window type = Hann, window size = 256 samples, 3 dB filter bandwidth = 270 Hz, brightness = 50%, contrast = 50%, overlap = 85% (locked), colour map = “Cool”, DFT size = 1024 samples (locked), grid spacing (spectral resolution) = 46.9 Hz. We analysed temporal traits in oscillograms and spectral traits in spectrograms (Köhler *et al.* 2017); we used the ‘Peak Frequency’ function to determine the peak of the dominant frequency. We generated sound figures through Seewave ver. 1.6 package (Sueur *et al.* 2008) and tuneR package (Ligges *et al.* 2018), R environment (ver. 3.3.1) (R Core Team 2017). The Seewave settings for the spectrograms were: Hanning window, 85% overlap, and 256 points resolution (FFT).

Phylogenetic tree and species-delimitation tests

The phylogenetic analyses were based on the Bayesian inference (BI) method. The dataset was composed of 149 terminals with 1045 characters from mitochondrial 16S ribosomal sequences, 892 characters from NADH dehydrogenase subunit 2 (*ND2*) sequences and 422 characters from Seven in Absentia Homolog 1 (*Siah*) sequences. We included the individuals assigned to *P. nordestinus* from the north and the south clades according to the dataset and topology of Bruschi *et al.* (2019) (see [Supplementary file 2](#)). To best evaluate the phylogenetic relationship status of the new species in comparison with sister species/taxa from the genus, we included sequences of at least three individuals (when available) of each of the species of *Pithecopus* deposited in GenBank (<https://www.ncbi.nlm.nih.gov/genbank> – see list of specimens in [Supplementary file 2](#)). *Callimedusa tomopterna* (Cope, 1868) was used as an outgroup because, according to Duellman *et al.* (2016), it represents a sister group of the clade which comprises the *Pithecopus* genus.

Bayesian inference was based on a Markov Monte Carlo (MCMC) analysis conducted on MrBayes 3:2.7 (Huelsenbeck & Ronquist 2001) with two independent runs, each run with four chains and sampling every 1000 generations for 20 million generations. MEGA X 10.1.8 (Kumar *et al.* 2018) selected the best evolutionary model through Akaike Information Criteria (AIC) (16S: *GTR + G*; *ND2*: *HKY + I + G*; *Siah*: *K2P*). The first 25% of the trees were excluded as burn-in. To confirm the quality of the parameters of the BI, Tracer software ver. 1.7.1 (Rambaut *et al.* 2018) was used, and only Effective Sample Sizes (ESS) values over 200 were considered acceptable.

We performed the Generalized Mixed Yule-Coalescent (GMYC) (Pons *et al.* 2006; Fontaneto *et al.* 2007) and the Poisson Tree Process (bPTP) (Zhang *et al.* 2013) methods to test species boundaries. The GMYC analysis requires an ultrametric tree that was estimated using a lognormal uncorrelated relaxed molecular clock model and coalescent constant size process, performed using BEAST ver. 1.10.4 (Drummond *et al.* 2012), with 20 million generations and sampling every 10 000 generations. The trees were estimated based on the HKY substitution model. We used the software Tracer ver. 1.7.1 (Rambaut *et al.* 2018) to check log files and all model parameters reached an ESS > 200. After removing 10% of the trees as part of the burn-in procedure, the remaining trees were summarized in a single tree with the Tree Annotator ver. 1.10.4 (Drummond *et al.* 2012). The GMYC analysis was carried out in R 3.6.1 software environment and performed with the packages Species Limits by Threshold Statistics ('splits') (Ezard *et al.* 2014) and Analyses of Phylogenetics and Evolution in R Language ('ape') (Paradis *et al.* 2018) using a single threshold and standard parameters [interval = c(0, 10)].

The bPTP does not require an ultrametric tree and uses the number of substitutions to model the speciation and coalescent events. For the analysis, the best maximum-likelihood (ML) tree reconstructed with RAxML (Kozlov *et al.* 2019) using an HKY model of nucleotide substitution selected with MEGA X 10.1.8 was used as input. The bPTP was performed on the web server (<http://species.h-its.org/>) for 5×10^5 generations, with a thinning value of 1000 and a burn-in of 10%.

Statistical analysis

Considering the morphological and acoustic (multivariate) datasets separately, we sought for discrimination between species by applying two functions in R environment: (1) randomForest (RF) (randomForest ver. 4.6-12 package) (Liaw & Wiener 2002) and (2) Discriminant Analysis on Principal Components (DAPC) (ade4 ver. 2.0.1 package; Jombart 2008; Jombart & Ahmed 2011). The same methods were applied in the description of *P. araguaius* (Haga *et al.* 2017a). RandomForest algorithm (machine learning) constructs many (e.g., 1000) classification trees using bootstrap samples of the data (each split using the best predictors among those randomly chosen at each node) then generating classifiers and aggregating results by voting to classes (Liaw & Wiener 2002). The classic Discriminant Analysis (DA) depends on multivariate normality (Pohar *et al.* 2004) and on a larger number of objects than variables. The multivariate normality of the original data was evaluated through the function mardiaTest (MVN package; Korkmaz *et al.* 2014). The DAPC performs analyses on the Principal Component scores (Jombart 2008; Jombart & Ahmed 2011). The application of a DA on a few axes (preserving about 95% of the variance) of a Principal Component Analysis, as performed by DAPC, reduces the sample-variable imbalance problems between objects and traits (Jombart *et al.* 2010).

For the multivariate analysis and statistical tests, we used all the morphometric features detailed above. For the acoustic analyses, we used: call duration (entire call), number of pulses, pulse duration, inter-pulse interval within core, core duration (main stronger group of pulses), pulses per core, pulses per second, isolated pulse and peak of dominant frequency. Because both multivariate analyses, to both datasets, were concordant in species discrimination (see Results), we present the results of RF classification only in tables and the results of DAPC only in scatter plots.

The acoustic and morphometric traits were tested for statistical significance of the differences among species through the Exact Wilcoxon-Mann-Whitney Rank Sum Test, function wilcox_test of the package Coin (resampling statistics model; Hothorn *et al.* 2008) in R environment. As these tests were done between species/populations pairs, the significance levels ('P') were adjusted considering the number of pairings through the P correction method of Holm (p.adjust function of the base package in R environment; see Chen *et al.* 2017). We considered significance when $P \leq 0.01$.

Results

Class Amphibia Linnaeus, 1758
Order Anura Fischer von Waldheim, 1813
Family Phyllomedusidae Günther, 1858
Genus *Pithecopus* Cope, 1866

Pithecopus gonzagai sp. nov.

[urn:lsid:zoobank.org:act:573D7AF0-0CB0-4D96-989E-EA3286190CB8](https://zoobank.org/urn:lsid:zoobank.org:act:573D7AF0-0CB0-4D96-989E-EA3286190CB8)

Figs 2–3; Tables 1–2

Phyllomedusa nordestina (only specimens from locations north of the SFR in the following studies) – Caramaschi 2006: 176–177, fig. 6. — Faivovich *et al.* 2010: 261, fig. 4, table 2. — Loebmann & Haddad 2010: 256, fig. 3, table 2. — Silva *et al.* 2010: 340, fig. 2, tables 1–2. — Toledo & Batista 2012: table S1. — Brand *et al.* 2013: 7065. — Neiva *et al.* 2013: 140. — Pinto *et al.* 2013: 656. — Toledo *et al.* 2015: 88, fig. 2. — Valencia-Aguilar *et al.* 2015: table 1. — Röhr *et al.* 2020: 653, fig. 2. *Pithecopus nordestinus* – Duellman *et al.* 2016: 91 (GenBank: GQ366016, GQ366091, GQ366143, GQ366330). — Dubeux *et al.* 2019: table 1; 2020: 15, figs 2, 10. — Silva *et al.* 2020: 165–172, fig. 1, tables 1, S1.

Diagnosis

Pithecopus gonzagai sp. nov. is assigned to the genus *Pithecopus* (former *Phyllomedusa hypochondrialis* species group; Caramaschi 2006) by the following set of characters: (1) small body size; (2) dorsolateral macroglands (*sensu* Antoniazzi *et al.* 2013) indistinct; (3) smooth skin on back and granulate on belly; (4) fingers and toes long and slender with terminal discs poorly developed; and (5) grasping (opposable to the others) finger I and toe I. *Pithecopus gonzagai* sp. nov. differs from the highland species of *Pithecopus* by the (6) lack of the reticulate pattern on flanks, and (7) head width smaller than 11.2 mm.

Etymology

The specific name honours Luiz Gonzaga do Nascimento, better known as Luiz Gonzaga. He was a Brazilian singer, songwriter, musician, poet and one of the most influential figures of Brazilian popular music in the twentieth century. Luiz Gonzaga has been credited for presenting the rich universe of north-eastern musical genres to the rest of the country. He was born and raised in the municipality of Exu, state of Pernambuco, Brazil. *Pithecopus gonzagai* sp. nov. also occurs in the state of Pernambuco, which is equally its type locality.

Type material

Holotype

BRAZIL • ♂ (Fig. 2); north-eastern Brazil, state of Pernambuco, municipality of Limoeiro; 7°52'29.0" S, 35°27'01.1" W; 150 m a.s.l.; 16 May 2011; D.P. Bruschi, M.A. Passos and Jonatha Lima leg.; ZUEC 19685.

Paratopotypes

BRAZIL • 23 ♂♂; same collection data as for holotype; ZUEC 19664 to 19668, 19670 to 19684, 19686 to 19688 • 4 ♀♀; same collection data as for holotype; ZUEC 19661 to 19663, 19669.

Other material examined

BRAZIL – Pernambuco • Limoeiro; ZUEC 19661 to 19688 • Bom Conselho; ZUEC 19617, 19619, 19622 to 19625, 19628 to 19633 • Caruaru; ZUEC 19610 to 19616 • Poção; ZUEC 19638, 19640 to 19644, 19646, 19649 to 19650, 19654 • Recife; ZUEC 19655 to 19660. – Alagoas • Pilar; ZUEC 19573,

19575, 19581 to 19582, 19584, 19587, 19590 to 19591, 19593 to 19594 • Rio Largo; ZUEC 19773, 19775, 19777, 19779, 19781 to 19783, 19785 to 19787 • São Miguel dos Campos; ZUEC 19565 to 19571 • São Miguel dos Milagres; 19595 to 19597, 19599 to 195604, 19606 to 19608 • Satuba; ZUEC 18627 to 18633, 18636 to 18638. – **Paraíba** • Araruna; ZUEC 19788, 19791, 19793, 19841 to 19842, 19848, 19854 • Cabaceiras; ZUEC 19689 to 19692, 19697 to 19699, 19702, 19704 to 19708, 19710 to 19711 • Campina Grande; ZUEC 19713 to 19722, 19724, 19729, 19732, 19733, 19734 • João Pessoa; 19726 to 19728, 19735 to 19740, 19743 • Mamanguape; ZUEC 19747, 19748, 19751, 19753, 19754 to 19756. – **Rio Grande do Norte** • Macaíba; ZUEC 19817, 19818, 19825, 19828, 19829, 19863 • São Paulo do Potengi; ZUEC 19805, 19811, 19834, 19846, 19851, 19853.

Description

Holotype

General aspect slender (Fig. 2A–B); snout truncate in dorsal and lateral views (Fig. 2C–D). Head wider than long; loreal region slightly concave; *canthus rostralis* rounded, smooth; nostrils small, subcanthal, placed latero-frontally, closer to snout tip than to eyes; internarial distance longer than eye-nostril distance and tympanum diameter, but smaller than eye diameter; eyes latero-frontally positioned; tympanum nearly circular, with annuli undefined at superior border; tympanum diameter less than half of eye diameter; supratympanic dermal fold present, beginning on right side of tympanum and ending near insertion of arm; dorsolateral macrogland indistinct; no external vocal sac; tongue nearly ovoid, free posteriorly, longer than wide, without pigmentation on base; vomerine teeth absent; choanae small, located laterally, slightly rounded. Upper arm thin and forearm robust; no finger webbing; comparative finger length when adpressed I < II < IV < III (Fig. 2E); finger discs poorly developed; finger I enlarged at base; nuptial asperity covering most of dorsal surface of finger I, except tip; palmar tubercles poorly developed, subarticular tubercles developed, barely distinguishable from adjacent supernumerary tubercles (Fig. 2E); inner and outer metacarpal tubercles poorly developed; comparative toe length when adpressed II < III < I < V < IV (Fig. 2F); toe webbing absent; plantar callosities poorly developed, inner and outer metatarsal tubercles poorly developed; subarticular tubercle developed, single and rounded; supernumerary tubercles rounded and poorly developed (Fig. 2F); legs slender; dorsal skin smooth; ventral skin granulated on belly, throat and thigh, smooth on tibia, tarsus and foot. Chest and right thigh slightly damaged ventrally due to tissue sampling. Cloacal region moderately granulated.

Measurements of holotype (mm)

SVL = 32.7, HL = 6.9 (21.1 % of SVL), HW = 9.8 (30.0 % of SVL), AGL = 15.6 (47.7 % of SVL), ED = 3.7 (11.3 % of SVL), TD = 1.2 (3.7 % of SVL), END = 2.2 (6.7 % of SVL), IND = 3.2 (9.8 % of SVL), UAL = 5.6 (17.1 % of SVL), FAL = 7.1 (21.7% of SVL), HAL = 8.1 (24.8 % of SVL), TGL = 12.7 (38.8 % of SVL), TL = 12.8 (39.1 % of SVL), TAL = 8.3 (25.4% of SVL) and FL = 10.9 (33.3 % of SVL).

Colouration in life

Dorsum of head and body green. Vertebral line on back present in some individuals (Fig. 3C), but absent in all individuals of the type series. Loreal region and eyelids green. Eyes outlined with thin white line. Edge of jaw bordered by black line. Green dorsal region delimited by white dorsolateral line extending from mouth end until around middle of axilla-groin length. Same white line also observed in distal parts of forelimbs, extending from elbow to end of finger IV. Black dorsolateral line (below white line) delimits ventral region; same line also found on forearms, tibia and foot portion. Anterior and posterior surfaces of upper arm, thigh and tibia, extending partially onto foot, orange with well-defined vertical black stripes. Forearm anterior surface extending to hand coloured orange with well-defined vertical black stripes. Orange inguinal region with well-defined vertical black stripes. Green dorsal surface extending onto all limbs: arm, forearm, thigh, knee and tibia; green dorsolateral surface of tarsus and foot (Fig. 3A–C).

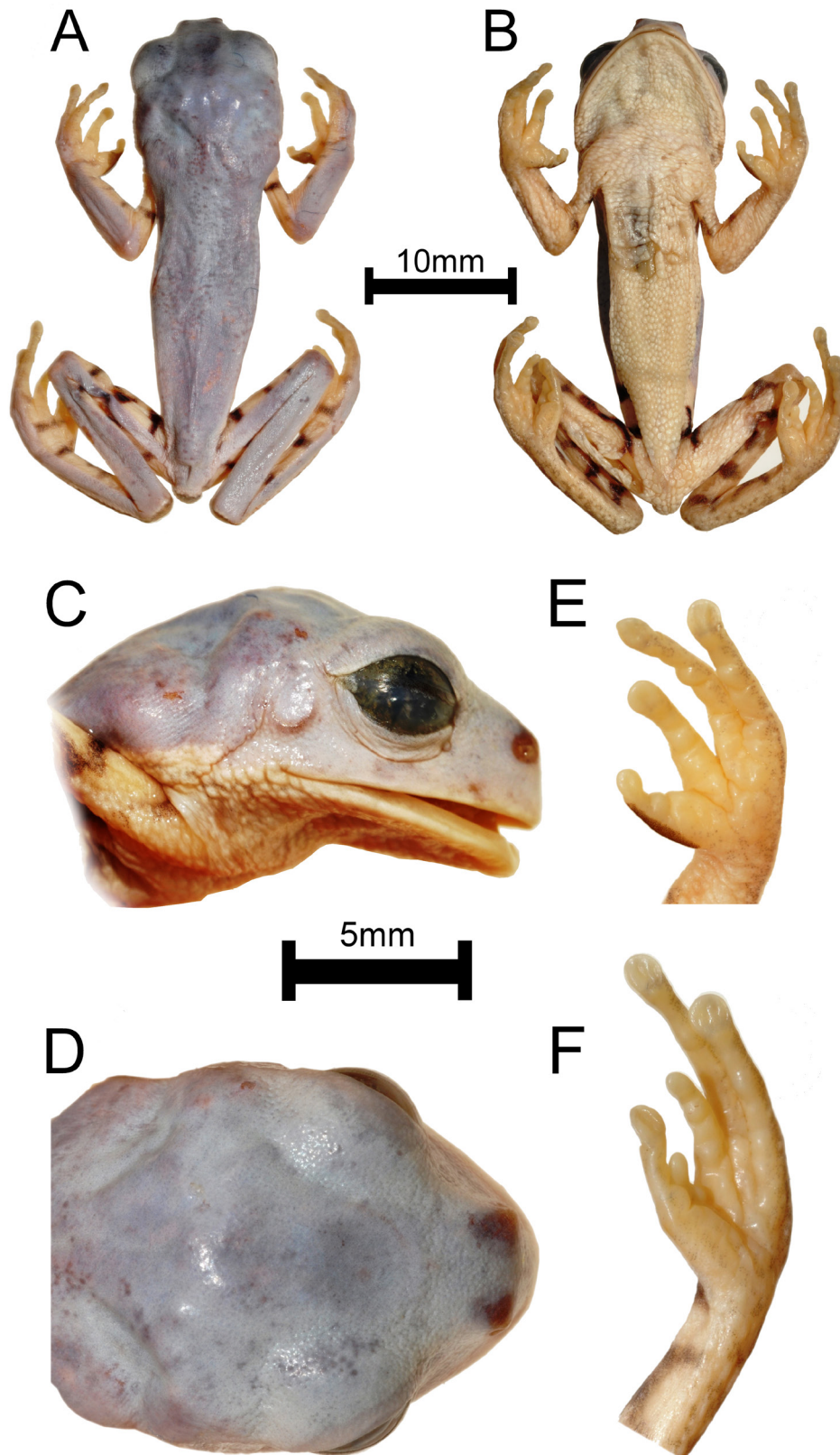


Fig. 2. *Pithecopus gonzagai* sp. nov., adult ♂, holotype (ZUEC 19685; SVL = 32.7 mm). **A.** Dorsal view. **B.** Ventral view. **C.** Head, lateral view. **D.** Head, dorsal view. **E.** Hand, ventral view. **F.** Foot, ventral view.

Variation in the type series

The specimens ZUEC 19661, 19663, 19667, 19669–70 and 19677–82 have slightly darkened blotches on back. The specimens ZUEC 19661–3, 19667 and 19669 have slightly darkened dots on back. The specimens ZUEC 19661–3, 19669–70, 19678–80 and 19688 have a well-defined dark stripe on edge of jaw (angular region). The specimens ZUEC 19664, 19668–9, 19673, 19675, 19680 and 19684 have slightly darkened terminal discs. Females larger than males, with robust body and lacking nuptial pads.

Differential diagnosis

Pithecopus gonzagai sp. nov. is promptly distinguished from *P. centralis*, *P. megacephalus*, *P. ayeaye*, *P. oreades* and *P. rusticus* by the absence of the reticulate pattern of colouration on flanks (Bokermann 1965; Lutz 1966; Brandão 2002; Caramaschi 2006; Bruschi *et al.* 2014). *Pithecopus gonzagai* sp. nov. is distinguished from *P. centralis* and *P. megacephalus* by its smaller head width (8.9–11.2 mm in *P. gonzagai* sp. nov. vs 12.2–14.5 mm, combined values for other species). Also, *P. gonzagai* sp. nov. differs from *P. ayeaye*, *P. megacephalus*, *P. oreades* and *P. rusticus* (9.9–12.7 mm, combined values) by its smaller head length (6.2–8.9 mm). The new species is distinguished from *P. centralis* and *P. megacephalus* (3.0–3.5 mm, combined values) by its smaller eye-nostril distance (1.8–2.8 mm) (Bokermann 1965;

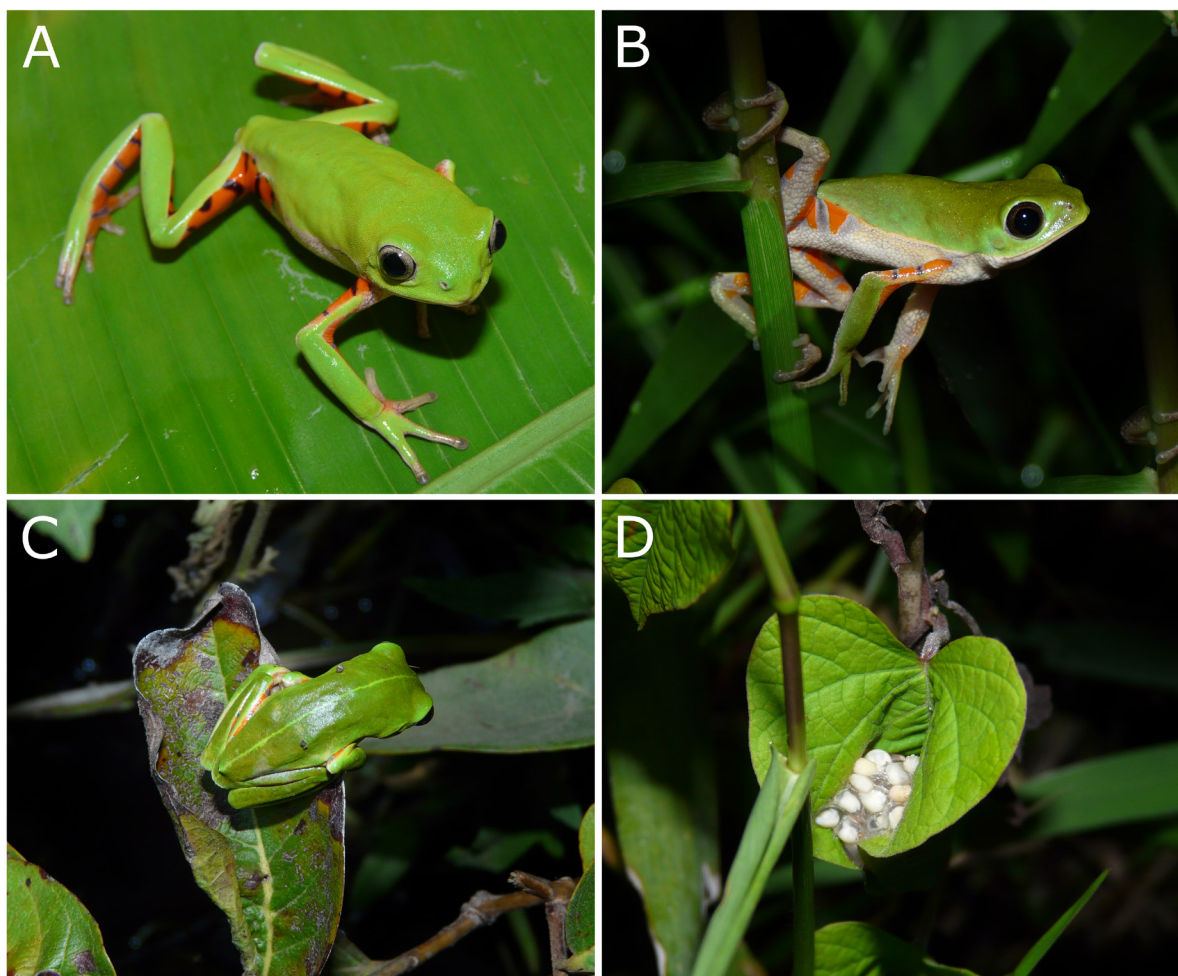


Fig. 3. *Pithecopus gonzagai* sp. nov. from Brazilian north-eastern, in life. **A.** From the municipality of Pilar, state of Alagoas (AL). **B.** From the municipality of Recife, state of Pernambuco (PE). **C.** From the municipality of São Miguel dos Milagres, AL. **D.** Arboreal eggs from the municipality of Poção, PE. Photographs by M. Aguiar.

Table 1. Morphometry of adult specimens of *Pithecopus gonzagai* sp. nov. (type series, 24 males including the holotype, and 150 individuals from 16 localities across four northeastern Brazilian states), and *P. nordestinus* (Caramaschi, 2006) (52 males including the holotype and 20 paratopotypes). Values presented in millimeters as mean \pm standard deviation (range); n = number of specimens measured.

| Traits | <i>P. gonzagai</i> sp. nov. | | | | <i>P. nordestinus</i> |
|----------------------|-------------------------------|-------------------------------|-------------------------------|-------------------------------|-------------------------------|
| | Type series | | Additional specimens | | Males |
| | Males n = 24 | Females n = 4 | Males n = 135 | Females n = 15 | n = 52 |
| Snout-vent length | 33.1 \pm 1.4 (29.5–35.3) | 38.0 \pm 0.8 (36.3–38.1) | 33.3 \pm 2.0 (28.5–37.8) | 37.9 \pm 1.6 (35.3–40.7) | 36.3 \pm 1.9 (32.9–42.5) |
| Head length | 7.6 \pm 0.7 (6.2–8.9) | 9.1 \pm 0.5 (7.8–9.1) | 7.3 \pm 0.5 (6.3–8.6) | 7.9 \pm 0.4 (7.3–8.6) | 7.5 \pm 0.7 (6.3–9.7) |
| Head width | 9.9 \pm 0.3 (9.1–10.4) | 11.9 \pm 0.4 (10.9–11.9) | 10.2 \pm 0.5 (8.9–11.2) | 11.4 \pm 0.5 (10.8–12.4) | 11.1 \pm 0.6 (9.9–12.7) |
| Axilla-groin length | 16.3 \pm 1.7 (12.6–18.8) | 19.1 \pm 1.3 (16.4–19.4) | 15.9 \pm 1.8 (11.8–19.5) | 18.5 \pm 1.9 (15.4–22.8) | 17.3 \pm 1.5 (14.5–20.8) |
| Eye diameter | 4.1 \pm 0.3 (3.6–4.6) | 4.8 \pm 0.4 (3.9–4.8) | 4.0 \pm 0.3 (3.0–4.9) | 4.4 \pm 0.3 (3.9–5.0) | 4.2 \pm 0.4 (3.3–4.9) |
| Tympanum diameter | 1.5 \pm 0.2 (1.2–1.8) | 2.2 \pm 0.3 (1.6–2.2) | 1.7 \pm 0.3 (1.1–2.3) | 1.9 \pm 0.2 (1.5–2.3) | 1.8 \pm 0.3 (1.2–2.3) |
| Eye-nostril distance | 2.1 \pm 0.2 (1.8–2.6) | 2.6 \pm 0.2 (2.0–2.5) | 2.3 \pm 0.2 (1.8–2.8) | 2.6 \pm 0.2 (2.3–3.0) | 2.5 \pm 0.2 (2.0–3.1) |
| Internarial distance | 3.1 \pm 0.3 (2.6–3.5) | 3.7 \pm 0.3 (3.1–3.7) | 3.0 \pm 0.3 (2.3–3.7) | 3.4 \pm 0.3 (2.9–3.8) | 3.4 \pm 0.3 (2.9–4.0) |
| Upper arm length | 6.2 \pm 0.4 (5.4–6.9) | 7.8 \pm 0.4 (7.0–7.9) | 6.7 \pm 0.6 (5.3–8.2) | 8.0 \pm 0.7 (6.6–9.0) | 7.3 \pm 0.5 (6.5–8.5) |
| Forearm length | 7.2 \pm 0.5 (6.3–8.0) | 9.8 \pm 0.6 (8.3–9.6) | 7.5 \pm 0.5 (6.3–8.8) | 9.3 \pm 0.6 (8.4–10.2) | 8.2 \pm 0.6 (6.9–9.3) |
| Hand length | 8.5 \pm 0.6 (7.7–9.9) | 11.0 \pm 0.9 (8.8–11.0) | 8.5 \pm 0.6 (7.0–9.7) | 9.8 \pm 0.6 (8.5–10.4) | 9.4 \pm 0.7 (8.0–11.2) |
| Thigh length | 13.5 \pm 0.7 (12.1–14.6) | 17.0 \pm 0.6 (15.8–17.2) | 14.1 \pm 0.8 (12.0–15.9) | 16.2 \pm 0.9 (14.6–18.0) | 15.1 \pm 0.8 (13.6–16.6) |
| Tibia length | 13.5 \pm 0.7 (11.9–14.8) | 16.5 \pm 0.6 (15.2–16.6) | 14.0 \pm 0.7 (12.4–16.0) | 16.0 \pm 0.8 (14.4–17.3) | 14.8 \pm 0.7 (13.4–16.2) |
| Tarsus length | 9.0 \pm 0.5 (8.1–9.9) | 11.0 \pm 0.4 (10.2–11.1) | 9.3 \pm 0.5 (7.9–10.5) | 10.4 \pm 0.6 (9.5–11.4) | 9.8 \pm 0.6 (8.8–11.1) |
| Foot length | 11.0 \pm 0.7 (9.6–12.6) | 13.4 \pm 0.7 (11.8–13.2) | 11.1 \pm 0.7 (9.5–12.9) | 12.8 \pm 0.8 (11.6–14.1) | 11.7 \pm 0.6 (10.4–13.1) |

Table 2. Advertisement call traits of two sister species of leaf frogs: *Pithecopus gonzagai* sp. nov. and *P. nordestinus* (Caramaschi, 2006). Values presented as mean \pm SD (range). * = mean of two isolated pulses; ** = mean of two inter-pulse intervals.

| Call traits | <i>P. gonzagai</i> sp. nov. n = 6 males/73 calls | <i>P. nordestinus</i> n = 6 males/105 calls |
|---|---|--|
| Call duration (ms) | 28.5 \pm 6.7 (17–49) | 51.0 \pm 8.5 (19–85) |
| Calls per minute | 34.9 \pm 17.1 (16.8–54.4) | 42.7 \pm 21.0 (11–82) |
| Pulses/call | 3.3 \pm 0.4 (3–4) | 4.0 \pm 1.0 (3–6) |
| Pulse duration (ms) | 7.3 \pm 1.3 (5–12) | 7.5 \pm 0.9 (3–16) |
| Inter-pulse interval within core (ms) | 0.9 \pm 0.7 (0–4) | 0.6 \pm 0.4 (0–6) |
| Core duration (ms) | 22.0 \pm 4.1 (17–35) | 24.2 \pm 2.2 (17–33) |
| Pulses/core | 3.0 \pm 0.0 (3–3) | 3.0 \pm 0.0 (3–4) |
| Duration of isolated pulses (ms) | 7.7 \pm 2.5 (4–12) | 8.3 \pm 1.7 (2–17)* |
| Number of isolated pulses | 1.0 (1–1) | 1.2 \pm 0.1 (1–2) |
| Interval between core and isolated pulse (ms) | 14.2 \pm 3.8 (8–22) | 17.2 \pm 4.7 (6–48)** |
| Pulses per second | 141.5 \pm 22 (86–177) | 127.0 \pm 11.7 (91–177) |
| Min. of dominant frequency (Hz) | 1,563 \pm 124 (1,188–1,927) | 1,508 \pm 126 (1,133–1,897) |
| Max. of dominant frequency (Hz) | 2,856 \pm 215 (2,446–3,592) | 2,539 \pm 260 (2,174–3,124) |
| Peak of dominant frequency (Hz) | 2,118 \pm 63.2 (1,969–2,391) | 2,074 \pm 47 (1,969–2,250) |
| Air temperature (°C) | 28.6 \pm 0.5 (28–29) | 24.6 \pm 3.0 (21–27) |
| Time of recording (hour:minutes) | 19:11–22:07 | 21:04–00:00 |

Lutz 1966; Brandão 2002; Caramaschi 2006; Bruschi *et al.* 2014). *Pithecopus gonzagai* sp. nov. is also distinguished from *P. centralis* (40.0–42.0 mm) by its smaller SVL (28.5–37.8 mm) (Bokermann 1965). The new species is distinguished from *P. rusticus* by the absence of the slightly reticulated pattern on the palpebral membrane and the throat region (pattern unique to *P. rusticus*; Bruschi *et al.* 2014).

From its closer relatives (the lowland species), *Pithecopus gonzagai* sp. nov. is distinguished by being smaller than *P. nordestinus*, *P. azureus* and *P. hypochondrialis* in SVL, head width and length of axilla-groin, internarial distance, and upper arm, hand, thigh, tibia and foot lengths (Exact Wilcoxon-Mann-Whitney Test: $P < 0.01$; see Table 3). In addition, based on P values obtained from the Exact Wilcoxon-Mann-Whitney Test (Table 3), *P. gonzagai* sp. nov. is smaller than *P. nordestinus* in eye-nostril distance (1.8–2.8 mm in the new species vs 2.0–3.1 mm in *P. nordestinus*), forearm length (6.3–8.8 mm in the new species vs 6.9–9.3 mm in *P. nordestinus*) and tarsus length (7.9–10.5 mm in the new species vs 8.8–11.1 mm in *P. nordestinus*). The new species is larger than *P. araguaeus* in SVL, head length, head width, axilla-groin and eye-nostril lengths, and upper arm, hand, thigh and foot lengths (see Table 3). The randomForest model on morphometric traits classified 90% of the males of the new species correctly (Table 4). It was the species with the highest percentage of males classified correctly in comparison with the other four taxa. DAPC based on morphological traits yielded no noticeable discrimination among the new species and *P. azureus*, *P. nordestinus* and *P. araguaeus* (Fig. 4A). However, it is possible to notice slight discrimination between the new species and *P. hypochondrialis* (Fig. 4A), with a greater separation along axis 1 (LD1 = 58%; axis x), but the axis 2 (LD2 = 25%; axis y) also contributes to the separation. Tarsus length (17%), head width (12%), tibia (12%) and foot (11%) lengths mainly accounted for species separation along LD1 (Fig. 4A); while tarsus (25%) and hand (16%) lengths, eye-

Table 3. *P*-values obtained using Exact Wilcoxon-Mann-Whitney Test based on morphometric comparisons between *Pithecopus gonzagai* sp. nov. (n = 159) and its closer relatives; *P* < 0.01 in bold. n = number of males measured. Further details on all males examined are in the Material and methods section and in the Appendix.

| Traits | vs <i>P. azureus</i> (n = 25) | vs <i>P. nordestinus</i> (n = 52) | vs <i>P. hypochondrialis</i> (n = 93) | vs <i>P. araguaius</i> (n = 36) |
|----------------------|----------------------------------|--------------------------------------|--|------------------------------------|
| Snout-vent length | 1.09 × 10⁻⁸ | 8.80 × 10⁻¹⁶ | 8.80 × 10⁻¹⁶ | 2.44 × 10⁻⁵ |
| Head length | 3.79 × 10 ⁻¹ | 3.79 × 10 ⁻¹ | 1.13 × 10⁻¹¹ | 1.40 × 10⁻³ |
| Head width | 5.32 × 10⁻⁵ | 8.80 × 10⁻¹⁶ | 8.80 × 10⁻¹⁶ | 4.50 × 10⁻⁹ |
| Axilla-groin length | 7.56 × 10⁻⁴ | 3.65 × 10⁻⁵ | 8.47 × 10⁻⁴ | 7.56 × 10⁻⁴ |
| Eye diameter | 5.89 × 10 ⁻¹ | 2.29 × 10 ⁻¹ | 1.25 × 10⁻¹⁵ | 2.42 × 10 ⁻¹ |
| Tympanum diameter | 9.43 × 10 ⁻¹ | 3.58 × 10 ⁻² | 1.06 × 10⁻³ | 8.56 × 10 ⁻¹ |
| Eye-nostril distance | 2.84 × 10 ⁻¹ | 3.26 × 10⁻¹¹ | 1.57 × 10⁻⁸ | 1.51 × 10⁻¹² |
| Internarial distance | 2.14 × 10⁻⁷ | 1.66 × 10⁻¹⁵ | 8.80 × 10⁻¹⁶ | 2.59 × 10 ⁻¹ |
| Upper arm length | 1.08 × 10⁻⁴ | 6.26 × 10⁻¹³ | 8.80 × 10⁻¹⁶ | 2.98 × 10⁻⁴ |
| Forearm length | 2.20 × 10 ⁻² | 5.87 × 10⁻¹⁴ | 8.80 × 10⁻¹⁶ | 9.33 × 10 ⁻¹ |
| Hand length | 8.29 × 10⁻⁵ | 1.29 × 10⁻¹² | 8.80 × 10⁻¹⁶ | 3.21 × 10⁻⁶ |
| Thigh length | 6.75 × 10⁻⁴ | 5.54 × 10⁻¹⁴ | 8.80 × 10⁻¹⁶ | 9.29 × 10⁻³ |
| Tibia length | 2.82 × 10⁻³ | 7.06 × 10⁻¹¹ | 8.80 × 10⁻¹⁶ | 2.50 × 10 ⁻² |
| Tarsus length | 2.19 × 10 ⁻¹ | 1.10 × 10⁻⁸ | 8.80 × 10⁻¹⁶ | 7.90 × 10 ⁻¹ |
| Foot length | 8.41 × 10⁻⁵ | 3.18 × 10⁻⁶ | 8.80 × 10⁻¹⁶ | 1.15 × 10⁻⁵ |

nostril distance (11%) and internarial distance (10%) accounted for the separation along LD2 (Fig. 4A). Morphometric measurements of all examined specimens and the eigenvectors of the DAPC based on morphometric traits are in [Supplementary files 3](#) and [4](#), respectively.

In comparison with the lowland species, the new species differs from *P. palliatus* by having the advertisement call with a higher dominant frequency (above 1900 Hz in *P. gonzagai* sp. nov. vs 1580 Hz in *P. palliatus*) and with a single note (= core portion) (double notes in *P. palliatus*; Köhler & Lötters 1999). Based on the Exact Wilcoxon-Mann-Whitney Test results, the new species can be distinguished from *P. hypochondrialis* and *P. araguaius* by having a lower number of pulses per advertisement call (new species: 3.3 ± 0.4 [3–4], *P. araguaius*: 6.0 ± 0.6 [5–8; *P* = 3.50 × 10⁻³], *P. hypochondrialis*: 4.2 ± 0.4 [3–6; *P* = 7.42 × 10⁻⁴]; present study; Haga *et al.* 2017a) and pulses per core (new species: 3.0 ± 0.0 [3–3], *P. araguaius*: 6.0 ± 0.5 [5–8; *P* = 3.50 × 10⁻³], *P. hypochondrialis*: 3.9 ± 0.3 [3–5; *P* = 2.61 × 10⁻⁶]; present study; Haga *et al.* 2017a), and shorter core duration (new species: 22.0 ± 4.1 [17–35 ms], *P. araguaius*: 39.3 ± 5.4 [28–48 ms; *P* = 3.50 × 10⁻³], *P. hypochondrialis*: 32.0 ± 4.0 [19–61 ms; *P* = 1.77 × 10⁻⁴]; present study; Haga *et al.* 2017a). In addition, the new species can also be differentiated from *P. araguaius* by the lower peak of the dominant frequency of its advertisement call (new species: 2118 ± 63.2 [1969–2391 Hz], *P. araguaius*: 2540 ± 308 [2240–3316 Hz; *P* = 4.66 × 10⁻³]; present study; Haga *et al.* 2017a), and from *P. hypochondrialis* by its shorter inter-pulse interval within the core (new species: 1.8 ± 0.8 [0–4 ms], *P. hypochondrialis*: 2.0 ± 1.0 [0–7 ms; *P* = 1.06 × 10⁻²]; present study; Haga *et al.* 2017a).

We were unable to find qualitative or quantitative diagnostic acoustic characters (absence of overlaps) between the new species, *P. nordestinus* and *P. azureus*. The randomForest model on acoustic traits was unable to distinguish one male of the new species from those of *P. hypochondrialis* (Table 4); the

Table 4. Confusion matrix for five of the lowland species of *Pithecopus* Cope, 1866 based on morphometric and **acoustic (values in bold)** datasets by means of a randomForest model. Settings: number of tree permutations = 1000; number of variables tried at each split = 3; error rates = 25.5 % | **10.9 %**.

| | <i>P. araguaius</i> | <i>P. azureus</i> | <i>P. gonzagai</i> sp. nov. | <i>P. hypochondrialis</i> | <i>P. nordestinus</i> | classification error |
|-----------------------------|---------------------|-------------------|--------------------------------|---------------------------|-----------------------|-------------------------|
| <i>P. araguaius</i> | 17 7 | 0 0 | 18 0 | 1 0 | 0 0 | 0.53 0.00 |
| <i>P. azureus</i> | 0 0 | 7 0 | 11 1 | 4 3 | 3 0 | 0.72 1.00 |
| <i>P. gonzagai</i> sp. nov. | 6 0 | 0 1 | 143 4 | 3 1 | 7 0 | 0.10 0.33 |
| <i>P. hypochondrialis</i> | 0 0 | 0 0 | 10 1 | 82 40 | 1 0 | 0.12 0.02 |
| <i>P. nordestinus</i> | 0 0 | 1 0 | 14 0 | 14 0 | 23 6 | 0.56 0.00 |

other five males were correctly classified. All six males of *P. nordestinus* were correctly classified. The univariate analyses did not recover differences between calls of the new species, *P. azureus* and *P. nordestinus*. In addition, there are overlaps in the acoustic traits of these three species. Among the lowland species, *P. araguaius* is the more acoustically distinct species (Fig. 4B). The greater separation among lowland species was along axis 1 (LD1 = 91%), while axis 2 contributed much less to the separation (LD2 = 7%). Pulses per core (30%), core duration (22%), isolated pulse (21%) and number of pulses per call (18%) mainly accounted for species separation along axis 1 (Fig. 4B). Eigenvectors of the DAPC based on acoustic traits are in [Supplementary file 5](#).

Phylogenetic inferences and species delimitation test

Bayesian inference was congruent with the phylogenetic intrageneric relations recovered by Faivovich *et al.* (2010), Duellman *et al.* (2016) and Haga *et al.* (2017a). In our topologies, we recovered two well-supported divergent clades (North and South) traditionally assigned to *P. nordestinus*, coincident with the phylogeographic breaks reported by Bruschi *et al.* (2019). The paratopotypes of *P. gonzagai* sp. nov. were recovered nested all with populations from north of SFR while the specimens of *P. nordestinus* were assembled with populations from south of SFR (Fig. 5, [Supplementary file 6](#)). The *P. gonzagai* sp. nov. + *P. nordestinus* are sister-group of the *P. azureus* (Fig. 5, [Supplementary file 6](#)).

The single-locus species discovery strategies by GMYC and bPTP approaches were performed in a dataset composed of 148 sequences consisting of 1049 nucleotides from mitochondrial DNA 16S gene, 134 sequences consisting of 892 nucleotides from *ND2* and 73 sequences consisting of 422 nucleotides from *Siah*. Both the GMYC and bPTP identified within the stringent threshold two taxonomic entities, congruent with two main lineages recovered by Bayesian inference (see Fig. 5, [Supplementary files 6, 7, 8, 9](#)).

Our results recovered same species clusters as shown by Bruschi *et al.* (2019) in a multi-locus study. GMYC analysis under an estimated ultrametric tree showed the threshold time (16S: -0.0001845922; *ND2*: -0.01166751; *Siah*: -0.0002401328) indicating the time all nodes reflect coalescent events; the likelihood of the null model was 1631.647 (16S), 1289.623 (*ND2*) and 644.3782 (*Siah*) and the maximum likelihood of the GMYC model was 1635.787 (16S), 1291.181 (*ND2*), 651.7409 (*Siah*). Because the differentiation among samples of *P. nordestinus* and *P. gonzagai* sp. nov. based on mitochondrial markers revealed high genetic distances level, the GMYC model suggested 52 entities composed of 32 distinct clusters for 16S, three entities composed of three clusters for *ND2* and 11 entities composed of ten clusters for *Siah*, however, with the exception of two individuals from Areia Branca, no mixture between samples of *P. nordestinus* and *P. gonzagai* sp. nov. was recovered in our inferences.

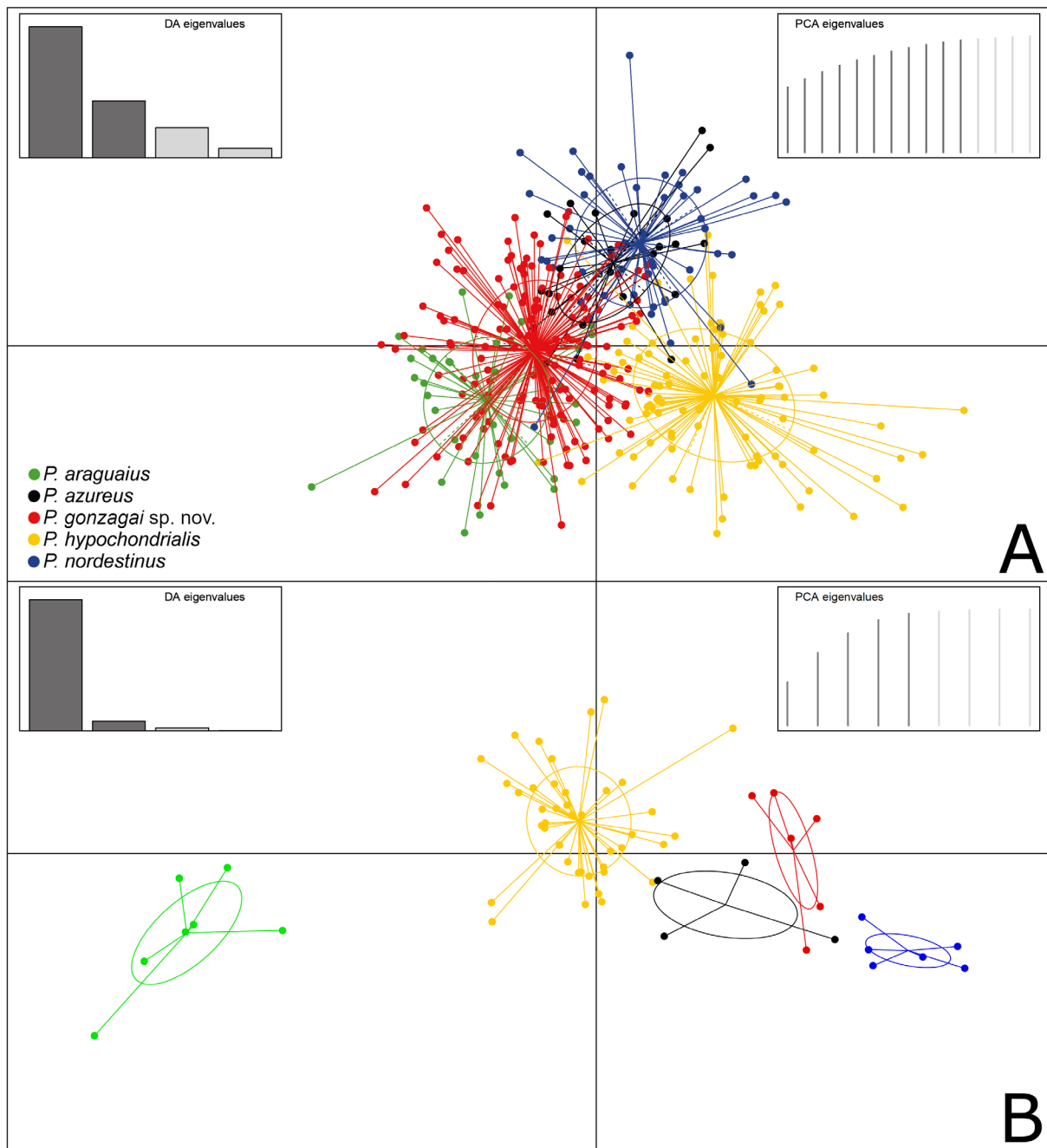


Fig. 4. Scatterplot of the discriminant analyses of principal components (DAPC) on the morphometric and acoustic datasets of *Pithecopus araguaeus* Haga *et al.*, 2017, *P. azureus* (Cope, 1862), *P. gonzagai* sp. nov., *P. hypochondrialis* (Daudin, 1800) and *P. nordestinus* (Caramaschi, 2006). **A.** The two first axes on the morphometric data (11 first PCs, 95% retained variance). Variance explained by the axes: LD1 = 58% (F-statistic = 131.7) and LD2 = 25% (F-statistic = 57.3). **B.** The two first axes on the acoustic data (5 first PCs, 96% retained variance). LD1 = 91% (F-statistic = 182.0) and LD2 = 7% (F-statistic = 13.5).

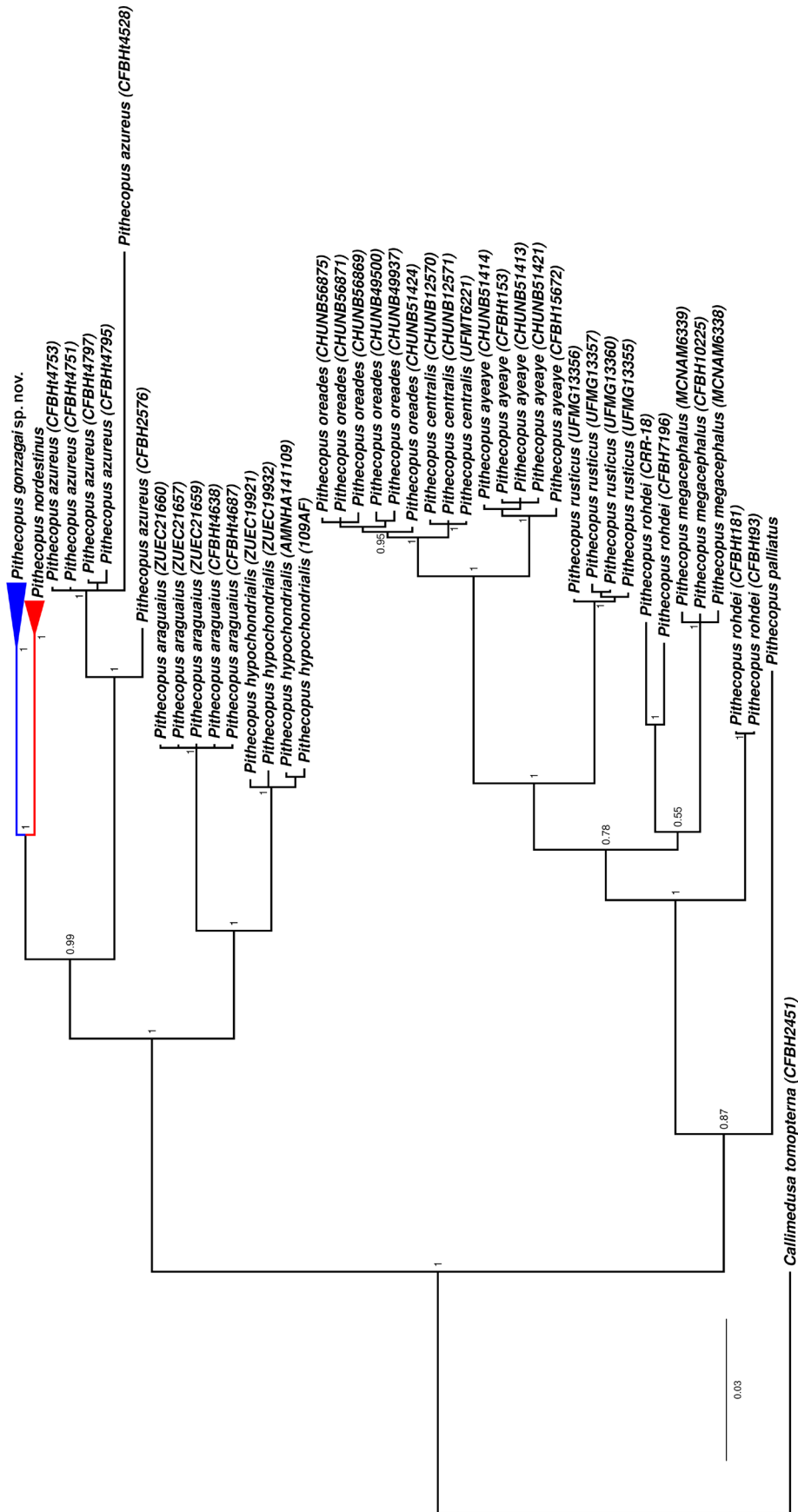


Fig. 5. Phylogenetic relationships of *Pithecopus* Cope, 1866 based on 16S rDNA mitochondrial fragment. Topology inferred from the Bayesian inference based on the *GTR+G* model. Posterior probabilities are shown at each node. Scale bar represents the number of substitutions per site. Expanded topology for *P. gonzagai* sp. nov. and *P. nordestimus* (Caramaschi, 2006) is in Supplementary file 6.

The tree resulting from the bPTP analysis recovered two species from the best ML search, completely separating individuals of the south (*P. nordestinus*) from individuals of the north (*Pithecopus gonzagai* sp. nov.). The highest Bayesian solution was similar to the ML tree; however, a total of 118 (16S), 85 (ND2) and 54 (*Siah*) putative entities were recovered by a simple heuristic search. In contrast, a mass sampling can contain individuals from real isolated clades and individuals in different states of structured populations, which may be the cause of the high number of entities found in the results from GMYC and bPTP analyses.

Advertisement call

Six males and 73 advertisement calls of the new species were recorded and analysed. Quantitative call traits are summarized in Table 2. The advertisement call of *P. gonzagai* sp. nov. consists of a single pulsed note emitted sporadically (Fig. 6A–B). The calls are generally composed of a main group of pulses (= core portion) (Fig. 6A), which may be followed by one low-amplitude final pulse (Fig. 6B). When present (37 % of analysed calls), the isolated pulses were limited to one and lasted 4–12 ms, separated from the core portion by a long interval of 8–22 ms. The pattern of three-pulsed core without the isolated pulse was more common (63% of analysed calls; Fig. 6A), and lasted 17–35 ms. Taking into account the isolated pulses, the call lasted 17–49 ms and has 3–4 pulses. The pulse duration varied from 5–12 ms, emitted at rates of 86–177 pulses/second. The inter-pulse interval (or no interval) within the core lasted 0–4 ms. The peak of dominant frequency varied from 1969 to 2391 Hz (Fig. 6A–B).

Six males and 105 advertisement calls of *P. nordestinus* (sister species) were recorded and analysed. The advertisement call of the sister species of the new taxon also contains a single pulsed note, with sporadic emission (quantitative call traits are summarized in Table 2; Fig. 6C–D). Core duration varied from 17 to 33 ms and the intervals between the core and the isolated pulses varied from 6 to 48 ms. The number of pulses per core varied from 3 to 4 pulses, with pulse intervals (or no interval) within the core from 0 to 6 ms. Pulses were arranged in: (1) a three-pulsed core with one isolated pulse (62.9%); (2) a three-pulsed core with no isolated pulse (16.2%); (3) a three-pulsed core followed by two isolated pulses, with long inter-pulse interval between them (17.1%; Fig. 6D); (4) a four-pulsed core followed by an isolated pulse (2.9%); and (5) a four-pulsed core followed by two isolated pulses, with long inter-pulse interval between them (1.0%). The entire call duration lasted 19–85 ms and has 3–6 pulses, the duration of which varied from 3 to 16 ms, emitted at rates of 91–177 pulses/second. The peak of dominant frequency varied from 1969–2250 Hz (Fig. 6D).

Distribution

Pithecopus gonzagai sp. nov. is known from the type locality and from the 16 municipalities in four north-eastern Brazilian states (Rio Grande do Norte, Paraíba, Pernambuco and Alagoas), based on molecular, acoustic and morphological evidence. It is possible that all populations occurring north of the SFR can be attributed to this new species, such as the populations from the states of Ceará and Piauí (Haddad *et al.* 2013; Roberto & Loebmann 2016); whereas all populations from south of the SFR (states of Sergipe and Bahia) are attributed to *P. nordestinus* (Fig. 1).

Natural history

Adult males of *P. gonzagai* sp. nov. call in the open areas, by the margins of lentic environments (mostly ponds) during the rainy season of the year (which could vary across its distribution). Females lay eggs on leaves over the water bodies (Fig. 3D), from where exotrophic tadpoles hatch and drop into the water. Therefore, the reproductive mode is the number 24 (*sensu* Haddad & Prado 2005). Different call types (advertisement, distress, warning and fighting calls) were described and previously attributed to *P. nordestinus* (see Toledo *et al.* 2015). However, part of those calls must now be attributed to *P. gonzagai* sp. nov.: the distress and warning calls described by Toledo *et al.* (2015) were recorded from individuals

sampled in the state of Rio Grande do Norte. Therefore, this population falls within the distribution of *P. gonzagai* sp. nov., not *P. nordestinus*. Thus, it is clear that both species (*P. nordestinus* and *P. gonzagai* sp. nov.) have a complex vocal repertoire that should be further explored.

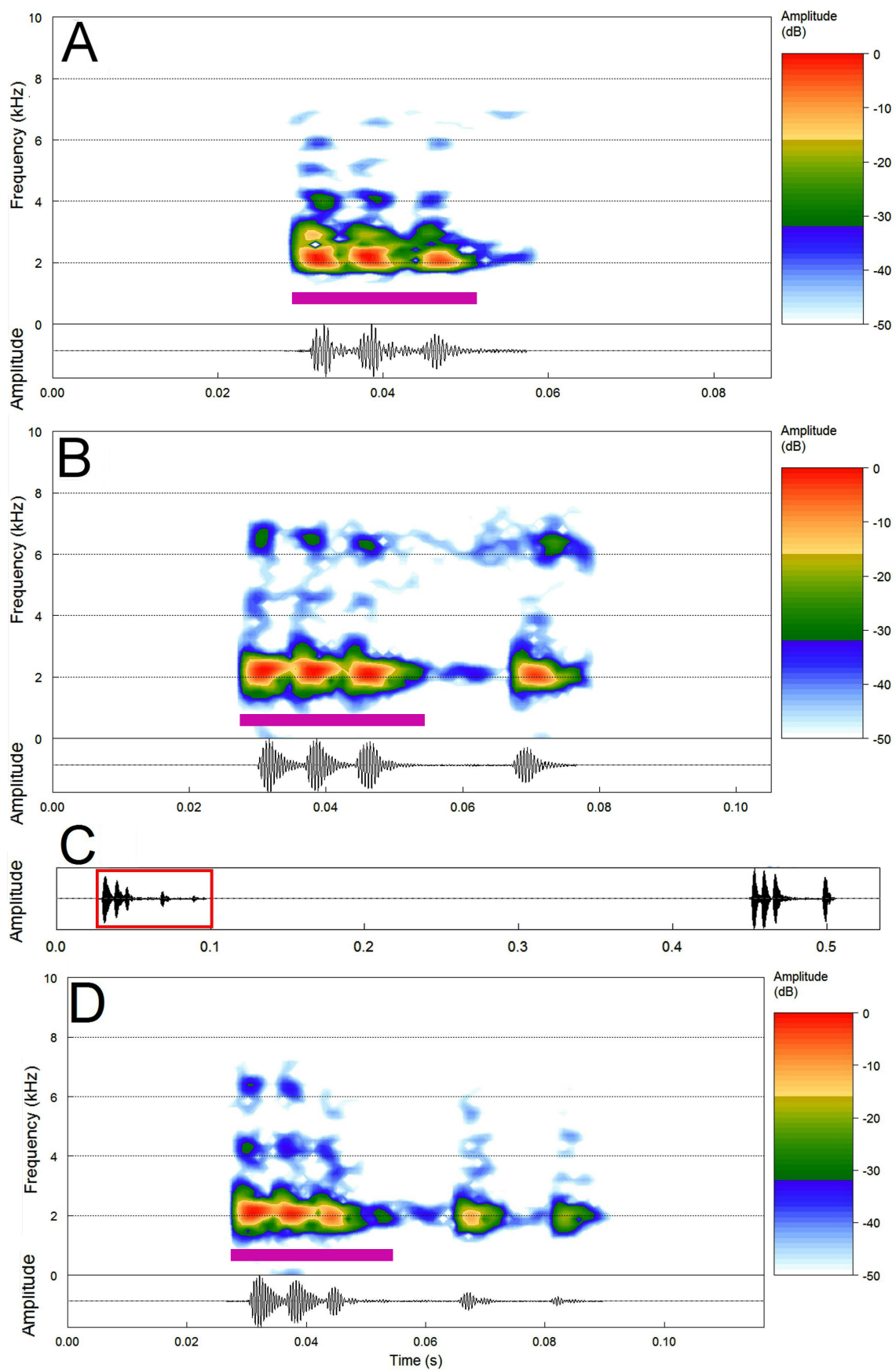
Conservation remarks

Besides corroborating previous observations, we draw attention to a recent governmental act to solve the water supply in semi-arid regions of north-eastern Brazil, the so-called São Francisco River Transposition Project. Already in progress, the transposition project is diverting water from SFR to temporary rivers and reservoirs of the polygon of droughts (called in Portuguese ‘polígono das secas’) (Lee 2009). This region is north of the SFR and suffers historically with the effects of prolonged droughts. In this project, there are two canals called the North and the East Axes (Fig. 1), which pump water from SFR to the driest regions when necessary (RIMA 2004). We may predict two possible impacts to the regional native fauna, including the present pair of species, *P. nordestinus* and *P. gonzagai* sp. nov.: a reduction of the geographic barrier effectiveness and/or even creation of new artificial barriers elsewhere. Therefore, the whole historical evolutionary dynamics of the species that inhabit this region would be modified. In the case of *P. gonzagai* sp. nov., its type locality and some others may be affected because they are between the new permanent and artificial rivers and the reduced SFR (Fig. 1). Therefore, we suggest a long-term genetic survey in this area to monitor the possible effects of the SFR Transposition Project.

Discussion

Our new species hypothesis was written under the ‘General Lineage Concept of Species’ (de Queiroz 1998, 2007), which treats species as separately evolving metapopulation lineages. We found significant differences in 12 morphometric traits when we compared *P. gonzagai* sp. nov. with *P. nordestinus*, the former being smaller in all traits. These traits corroborate phylogenetic evidence (Bruschi *et al.* 2019) and species delimitation tests showed here. As *P. gonzagai* sp. nov. is a phenotypically cryptic species, we are unable to indicate a reliable phenotypic diagnostic character to distinguish it from *P. nordestinus*. That is why *P. gonzagai* sp. nov. has been historically masked by its phenotypic similarity with *P. nordestinus* (Caramaschi 2006; Loebmann & Haddad 2010; Brand *et al.* 2013; Pinto *et al.* 2013; Neiva *et al.* 2013). The ancient interruption of the gene flow due to a historical shift in the course of SFR is the best explanation for the *P. nordestinus* and *P. gonzagai* sp. nov. split from their most recent common ancestor during the Plio-Pleistocene transition (Bruschi *et al.* 2019). Despite the clear split between *P. nordestinus* and *P. gonzagai* sp. nov., samples from Catieté and Aurelino Leal (Western Bahia state) could represent a putative secondary contact zone between the two species (Bruschi *et al.* 2019) or the signature of incomplete lineage sorting. The cyto-nuclear noise detected in Western Bahia

Fig. 6 (next page). Spectrograms (above) and oscillograms (below) of the advertisement call of *Pithecopus gonzagai* sp. nov. (A–B) and *P. nordestinus* (Caramaschi, 2006) (C–D). **A.** Spectrogram and corresponding oscillogram of the call of *P. gonzagai* sp. nov. with no isolated pulse, just the core, from the type locality, municipality of Limoeiro, state of Pernambuco, 17 May 2011, 19:35, air temperature 28°C (FNJV 12231). **B.** Spectrogram and corresponding oscillogram of the call of *P. gonzagai* sp. nov. with one isolated low-amplitude pulse after the core, recorded in the municipality of Araruna, state of Paraíba, 22 May 2011, 20:45, air temperature 29°C (FNJV 12233). **C.** Oscillogram of two advertisement calls of *P. nordestinus*: the first with two isolated low-amplitude pulses after the core, and the second without isolated pulses (FNJV 12244). **D.** Spectrogram and corresponding oscillogram of the advertisement call of *P. nordestinus* from the section highlighted in red in C, recorded in the municipality of Areia Branca, state of Sergipe, 5 May 2011, 21:22, air temperature 27°C (FNJV 12244). Purple lines highlight the cores of the calls.



requires further study, including more comprehensive sampling, to evaluate the source of this genetic signal.

Indeed, the routine morphological identification of the species of *Pithecopus* is not easy mostly due to the high level of conservative morphology observed between *P. hypochondrialis*, *P. azureus* and *P. nordestinus* (Bruschi *et al.* 2013; Haga *et al.* 2017a). It is noteworthy that *P. azureus* and *P. nordestinus* are also morphometrically indistinguishable from one another according to the present analysis and those carried out by Haga *et al.* (2017a). Moreover, acoustic traits used in our analysis did not discriminate the new species from *P. nordestinus* and *P. azureus*. However, these three allopatric species are currently isolated by geographical barriers (Bruschi *et al.* 2013, 2019; Haga *et al.* 2017a). If we consider the allopatry and that the phenotypic divergence is fuelled by the joint influence of character displacement and sexual selection (see Pfennig & Pfennig 2010), the selective pressures acting on call traits could be very weak or simply non-existent.

In addition, Haga *et al.* (2017b) pointed out that the similarities observed among the advertisement calls of *P. hypochondrialis*, *P. azureus* and *P. nordestinus* (the lowland species), and the resulting difficulty in discriminating them, indicate that acoustic traits are uninformative for these phylogenetically closely related species. All six males of *P. nordestinus* were correctly classified in the randomForest model. This discrepancy can probably be explained by the fact that calls with two isolated pulses were only reported for *P. nordestinus*. The other five lowland species have, at most, one isolated pulse following the core portion. Although we have found significant differences in some acoustic traits, there are overlaps in their amplitudes, which may affect the specific recognition by females of these lowland species. Moreover, we were unable to find clear acoustic diagnosis between the two sister highland species, *P. oreades* and *P. centralis*, as there are overlaps in all their acoustic traits (Brandão & Álvares 2009; Brandão *et al.* 2009). Therefore, as well as for *P. gonzagai* sp. nov. and *P. nordestinus*, the acoustic traits are not useful to distinguish other related species of *Pithecopus*. Also, populations of *P. nordestinus* and *P. gonzagai* sp. nov. from the Atlantic Rainforest and from the Caatinga showed differences in the interval between the pulses of the advertisement call, revealing putative intraspecific variation (Röhr *et al.* 2020). The authors pointed out that their results indicate how multiple evolutionary forces may act simultaneously on the advertisement calls of frogs (Röhr *et al.* 2020).

A characterisation of tadpoles of *P. nordestinus* was recently provided (Dubeux *et al.* 2020). However, this study analysed individuals collected north of the SFR (states of Alagoas and Rio Grande do Norte), therefore, *P. gonzagai* sp. nov. is the most suitable taxonomic identification for these tadpoles characterised by Dubeux *et al.* (2020), not *P. nordestinus*. The advertisement call of *P. nordestinus* described from the municipality of Igrapiúna, state of Bahia (about 145 km northwest of the type locality) is similar to those described here in call duration, pulse duration and dominant frequency but slightly different in number of notes per call and inter-pulse interval (see Vilaça *et al.* 2011). Possibly, these differences can be explained by an intraspecific variation or even an applied methodology, since the molecular data indicate that the populations south of the SFR correspond to *P. nordestinus*. Using species distribution modelling algorithms and based on direct field sampling, scientific literature, museum collections, and available online databases, Silva *et al.* (2020) provided a new distribution area for *P. nordestinus* which was broader than previously known. In addition, these same authors suggested a new polygon for conservation purposes for this species. In contrast, the distribution suggested by them overlaps with the geographic distributions of *P. nordestinus* and *P. gonzagai* sp. nov. reported by Bruschi *et al.* (2019) and the present study.

Pithecopus gonzagai sp. nov. and *P. nordestinus* are examples that fulfil the definition for cryptic species of Bickford *et al.* (2007): “two or more distinct species that are erroneously classified (and hidden) under one species name”. The identification of cryptic species complexes allows us to better plan biodiversity

conservation strategies (Bickford *et al.* 2007). Thus, the description of *P. gonzagai* sp. nov. as a new species has a direct impact for conservation planning on a regional scale. Future projects evaluating north-eastern diversity are needed to identify cryptic species that may be divided by the natural course of the São Francisco River.

Acknowledgements

We thank to M.A. Passos, A.A. Giaretta, L.B. Martins, T. Vilaça and T.R. de Carvalho, who kindly made available their recordings. M. Aguiar provided pictures of live individuals of the new species. A.A. Giaretta, J.P. Pombal Jr. and C.F.B. Haddad gave access to the specimens under their care. We thank to D. Baêta and an anonymous reviewer for their insightful comments during the review process. Coordenação de Aperfeiçoamento de Pessoal de Nível Superior (CAPES) provided MSc fellowships to IAH and FSA. São Paulo Research Foundation (FAPESP) provided a PhD scholarship to FSA (Process #2015/10728-7) and grants to LFT (#2016/25358-3; #2019/18335-5), DPB and SMRP (#2016/07717-6). Conselho Nacional de Desenvolvimento Científico e Tecnológico (CNPq) provided a fellowship (#300896/2016-6) to LFT. IAH and FSA thank the Cornell Lab of Ornithology (Bioacoustics Research Program) for providing free licenses of Raven Pro.

References

- Antoniazzi M.M., Neves P.R., Mailho-Fontana P.L., Rodrigues M.T. & Jared C. 2013. Morphology of the parotoid macroglands in *Phyllomedusa* leaf frogs. *Journal of Zoology* 291 (1): 42–50. <https://doi.org/10.1111/jzo.12044>
- Bickford D., Lohman D.J., Sodhi N.S., Ng P.K.L., Meier R., Winker K., Ingram K.K. & Das I. 2007. Cryptic species as a window on diversity and conservation. *TRENDS in Ecology and Evolution* 22 (3): 148–155. <https://doi.org/10.1016/j.tree.2006.11.004>
- Bioacoustics Research Program. 2014. *Raven Pro: Interactive Sound Analysis Software, version 1.5*. The Cornell Lab of Ornithology, Ithaca, New York. Available from <http://www.birds.cornell.edu/raven> [accessed 5 Feb. 2015].
- Bokermann W.C.A. 1965. Três novos batráquios da região central de Mato Grosso. *Brazilian Journal of Biology* 25: 257–264.
- Brand G.D., Santos R.C., Arake L.M., Silva V.G., Veras L.M.C., Costa V., Costa C.H.N., Kuckelhaus S.S., Alexandre J.G., Feio M.J. & Leite J.R.S.A. 2013. The skin secretion of the amphibian *Phyllomedusa nordestina*: a source of antimicrobial and antiprotazoal peptides. *Molecules* 18: 7058–7070. <https://doi.org/10.3390/molecules18067058>
- Brandão R.A. 2002. A new species of *Phyllomedusa* Wagler, 1830 (Anura: Hylidae) from central Brazil. *Journal of Herpetology* 36 (4): 571–578. <https://doi.org/10.2307/1565926>
- Brandão R.A. & Álvares G.F.R. 2009. Remarks on a new *Phyllomedusa* Wagler (Anura: Hylidae) with reticulated pattern on flanks from Southeastern Brazil. *Zootaxa* 2044: 61–64. <https://doi.org/10.11646/zootaxa.2044.1.4>
- Brandão R.A., Álvares G.F.R., Crema A. & Zerbini G.J. 2009. Natural history of *Phyllomedusa centralis* Bokermann 1965 (Anura: Hylidae: Phyllomedusinae): tadpole and calls. *South American Journal of Herpetology* 4: 61–68. <https://doi.org/10.2994/057.004.0108>
- Bruschi D.P., Busin C.S., Toledo L.F., Vasconcellos G.A., Strussmann C., Weber L.N., Lima A.P., Lima J.D. & Recco-Pimentel S.M. 2013. Evaluation of the taxonomic status of populations assigned to *Phyllomedusa hypochondrialis* (Anura, Hylidae, Phyllomedusinae) based on molecular, chromosomal, and morphological approach. *Genetics* 14 (70): 1–14. <https://doi.org/10.1186/1471-2156-14-70>

Bruschi D.P., Lucas E.M., Garcia P.C. & Recco-Pimentel S.M. 2014. Molecular and morphological evidence reveals a new species in the *Phyllomedusa hypochondrialis* group (Hylidae, Phyllomedusinae) from the Atlantic Forest of the highlands of southern Brazil. *PLoS ONE* 9 (8): e105608.

<https://doi.org/10.1371/journal.pone.0105608>

Bruschi D.P., Peres E.A., Lourenço L.B., Bartoletti L.F.M., Sobral-Souza T. & Recco-Pimentel S.M. 2019. Signature of the paleo-course changes in the São Francisco River as source of genetic structure in Neotropical *Pithecopus nordestinus* (Phyllomedusinae, Anura) treefrog. *Frontiers in Genetics* 10: 728.

<https://doi.org/10.3389/fgene.2019.00728>

Caramaschi U. 2006. Redefinição do grupo de *Phyllomedusa hypochondrialis*, com redescritção de *P. megacephala* (Miranda-Ribeiro, 1926), revalidação de *P. azurea* Cope, 1862 e descrição de uma nova espécie (Amphibia, Anura, Hylidae). *Archivos do Museu Nacional do Rio de Janeiro* 64 (2): 159–179.

Chen S.Y., Feng Z. & Yi X. 2017. A general introduction to adjustment for multiple comparisons. *Journal of Thoracic Disease* 9 (6): 1725–1729. <https://doi.org/10.21037/jtd.2017.05.34>

Clemente-Carvalho R.B.G., Giaretta A.A., Condez T.H., Haddad C.F.B. & Reis S.F.D. 2012. A new species of miniaturized toadlet, genus *Brachycephalus* (Anura: Brachycephalidae), from the Atlantic Forest of southeastern Brazil. *Herpetologica* 68 (3): 365–374.

<https://doi.org/10.1655/HERPETOLOGICA-D-11-00085.1>

de Queiroz K. 1998. The general lineage concept of species, species criteria, and the process of speciation and terminological recommendations. In: Howard D.J. & Berlocher S.H. (eds) *Endless Forms: Species and Speciation*: 57–75. Oxford University Press, Oxford.

de Queiroz K. 2007. Species concepts and species delimitation. *Systematic Biology* 56 (6): 879–886. <https://doi.org/10.1080/10635150701701083>

Dubeux M.J.M., Silva G.R.S., Nascimento F.A.C., Gonçalves U. & Mott T. 2019. Síntese histórica e avanços no conhecimento de girinos (Amphibia: Anura) no estado do Alagoas, nordeste do Brasil. *Revista Nordestina de Zoologia* 12: 18–52.

Dubeux M.J.M., Nascimento F.A.C., Lima L.R., Magalhães F.M., Silva I.R., Gonçalves U., Almeida J.P.F., Correia L.L., Garda A.A., Mesquita D.O., Rossa-Feres D.C. & Mott T. 2020. Morphological characterization and taxonomic key of tadpoles (Amphibia: Anura) from the northern region of the Atlantic Forest. *Biota Neotropica* 20 (2): e20180718. <https://doi.org/10.1590/1676-0611-BN-2018-0718>

Duellman W.E. 1970. *The Hylid Frogs of Middle America. Vol. 1*. Monograph of the Museum of Natural History 1, University of Kansas, Lawrence. <https://doi.org/10.5962/bhl.title.2835>

Duellman W.E., Marion A.B. & Hedges S.B. 2016. Phylogenetics, classification, and biogeography of the treefrogs (Amphibia: Anura: Arboranae). *Zootaxa* 4104 (1): 001–109.

<https://doi.org/10.11646/zootaxa.4104.1.1>

Drummond A.J., Suchard M.A. & Rambaut A. 2012. Bayesian phylogenetics with BEAUti and the BEAST 1.7. *Molecular Biology and Evolution* 29 (8): 1969–1973. <https://doi.org/10.1093/molbev/mss075>

Ezard T.H.G., Fujisawa T.E. & Barraclough T.G. 2014. *splits: SPecies' Limits by Threshold Statistics. R package version 1.0-19/r51*. Available from <https://R-Forge.R-project.org/projects/splits/> [assessed 21 Mar. 2020].

Faivovich J., Haddad C.F.B., Baêta D., Jungferd K.H., Alvares G.F.R., Brandão R.A., Sheil C., Barrientos L.S., Barrio-Amorós C.L., Cruz C.A.G. & Wheeler W.C. 2010. The phylogenetic relationships of the charismatic poster frogs, Phyllomedusinae (Anura, Hylidae). *Cladistics* 26 (3): 227–261.

<https://doi.org/10.1111/j.1096-0031.2009.00287.x>

- Fišer C., Robinson C.T. & Malard F. 2018. Cryptic species as a window into the paradigm shift of the species concept. *Molecular Ecology* 27 (3): 613–635. <https://doi.org/10.1111/mec.14486>
- Fontaneto D., Herniou E., Boschetti C., Caprioli M., Melone G., Ricci C. & Barraclough T.G. 2007. Independently evolving species in asexual bdelloid rotifers. *Plos Biology* 5: e87. <https://doi.org/10.1371/journal.pbio.0050087>
- Frost D.R. 2020. *Amphibian Species of the World: an Online Reference. Ver. 6.0*. American Museum of Natural History, New York. Available from <http://research.amnh.org/herpetology/amphibia/index.html> [accessed 3 Apr. 2020].
- Haddad C.F.B. & Prado C.P. 2005. Reproductive modes in frogs and their unexpected diversity in the Atlantic Forest of Brazil. *BioScience* 55 (3): 207–217. [https://doi.org/10.1641/0006-3568\(2005\)055\[0207:RMIFAT\]2.0.CO;2](https://doi.org/10.1641/0006-3568(2005)055[0207:RMIFAT]2.0.CO;2)
- Haddad C.F.B., Toledo L.F., Prado C.P.A., Loebmann D., Gasparini J.L. & Sazima I. 2013. *Guide to the Amphibians of the Atlantic Forest: Diversity and Biology. First Edition*. Anolis Books, São Paulo.
- Haga I.A., Andrade F.S., Bruschi D.P., Recco-Pimentel S.M. & Giaretta A.A. 2017a. Unrevealing the leaf frogs Cerrado diversity: a new species of *Pithecopus* (Anura, Arboranae, Phyllomedusidae) from the Mato Grosso state, Brazil. *PLoS ONE* 12 (9): e0184631. <https://doi.org/10.1371/journal.pone.0184631>
- Haga I.A., Carvalho T.R., Andrade F.S. & Giaretta A.A. 2017b. Advertisement and aggressive calls of *Pithecopus azureus* (Anura: Phyllomedusidae) from the border of Brazil and Paraguay. *Phyllomedusa* 16 (1): 47–56. <https://doi.org/10.11606/issn.2316-9079.v16i1p47-56>
- Huelsenbeck J.P. & Ronquist F. 2001. MRBAYES: Bayesian inference of phylogeny. *Bioinformatics* 17: 754–755. <https://doi.org/10.1093/bioinformatics/17.8.754>
- Hothorn T., Hornik K., Van de Wiel M.A. & Zeileis A. 2008. Implementing a class of permutation tests: the coin package. *Journal of Statistical Software* 28 (8): 1–23. <https://doi.org/10.18637/jss.v028.i08>
- Jombart T. 2008. *adeigenet*: a R package for the multivariate analysis of genetic markers. *Bioinformatics* 24: 1403–1405. <https://doi.org/10.1093/bioinformatics/btn129>
- Jombart T. & Ahmed I. 2011. *adeigenet 1.3-1*: new tools for the analysis of genome-wide SNP data. *Bioinformatics* 27 (21): 3070–3071. <https://doi.org/10.1093/bioinformatics/btr521>
- Jombart T., Devillard S. & Balloux F. 2010. Discriminant analysis of principal components: a new method for the analysis of genetically structured populations. *Genetics* 11: 1–15. <https://doi.org/10.1186/1471-2156-11-94>
- Köhler J. & Lötters S. 1999. Annotated list of amphibian records from the Departamento Pando, Bolivia, with description of some advertisement calls. *Bonner zoologische Beiträge* 48: 259–273.
- Köhler J., Jansen M., Rodríguez A., Kok P.J.R., Toledo L.F., Emmrich M., Glaw F., Haddad C.F.B., Rödel M.O. & Vences M. 2017. The use of bioacoustics in anuran taxonomy: theory, terminology, methods and recommendations for best practice. *Zootaxa* 4251: 1–124. <https://doi.org/10.11646/zootaxa.4251.1.1>
- Korkmaz S., Goksuluk D. & Zararsiz G. 2014. MVN: an R package for assessing multivariate normality. *The R Journal* 6 (2): 151–163. <https://doi.org/10.32614/RJ-2014-031>
- Kozlov A.M., Darriba D., Flouri T., Morel B. & Stamatakis A. 2019. RAXML-NG: a fast, scalable, and user-friendly tool for maximum likelihood phylogenetics inference. *Bioinformatics* 35 (21): 4453–4455. <https://doi.org/10.1093/bioinformatics/btz305>
- Kumar S., Stecher G., Li M., Knyas C. & Tamura K. 2018. MEGA X: Molecular genetics analysis across computing platforms. *Molecular Biology and Evolution* 35 (6): 1547–1549. <https://doi.org/10.1093/molbev/msy096>

- Lee J. 2009. The São Francisco River Transposition Project: friend or foe to the Brazilian people. *Law and Business Review of the Americas* 15: 425–434.
- Liaw A. & Wiener M. 2002. Classification and regression by randomForest. *R News* 2 (3): 18–22.
- Ligges U., Krey S., Mersmann O. & Schnackenberg S. 2018. *tuneR: Analysis of Music and Speech*. Available from <https://CRAN.R-project.org/package=tuneR> [accessed 1 Jul. 2018].
- Loebmann D. & Haddad C.F.B. 2010. Amphibians and reptiles from a highly diverse area of the Caatinga domain: composition and conservation implications. *Biota Neotropica* 10 (3): 227–256. <https://doi.org/10.1590/S1676-06032010000300026>
- Lutz B. 1966. *Pithecopus ayeaye*, a new Brazilian hylid with vertical pupils and grasping feet. *Copeia* 48: 236–240. <https://doi.org/10.2307/1441130>
- Neiva M., Vargas D.C., Conceição K., Rádis-Baptista G., Assakura M.T., Jared C. & Hayashi M.A.F. 2013. Gene expression analysis by ESTs sequencing of the Brazilian frog *Phyllomedusa nordestina* skin glands. *Toxicon* 61: 139–150. <https://doi.org/10.1016/j.toxicon.2012.10.016>
- Paradis E. & Schliep K. 2018. ape 5.0: an environment for modern phylogenetics and evolutionary analyses in R. *Bioinformatics* 35: 526–528. <https://doi.org/10.1093/bioinformatics/bty633>
- Pfennig D.W. & Pfennig K.S. 2010. Character displacement and the origins of diversity. *The American Naturalist* 176: S26–S44. <https://doi.org/10.1086/657056>
- Pinto E.G., Pimenta D.C., Antoniazzi M.M., Jared C. & Tempone A.G. 2013. Antimicrobial peptides isolated from *Phyllomedusa nordestina* (Amphibia) alter the permeability of plasma membrane of *Leishmania* and *Trypanosoma cruzi*. *Experimental Parasitology* 135: 655–660. <https://doi.org/10.1016/j.exppara.2013.09.016>
- Pohar M., Blas M. & Turk S. 2004. Comparison of logistic regression and linear discriminant analysis: a simulation study. *Metodološki zvezki* 1 (1): 143–161.
- Pons J., Barraclough T.G., Gomez-Zurita J., Cardoso A., Duran D.P. & Hazell S. 2006. Sequence-based species delimitation for the DNA taxonomy of undescribed insects. *Systematic Biology* 55: 595–609. <https://doi.org/10.1080/10635150600852011>
- R Core Team. 2017. *R: a Language and Environment for Statistical Computing*. Ver. 3.1.2. R Foundation for Statistical Computing, Vienna. Available from <http://www.R-project.org/> [accessed 1 Jul. 2017].
- Rambaut A., Drummond A.J., Xie D., Baele G. & Suchard M.A. 2018. Posterior summarization in Bayesian phylogenetics using Tracer 1.7. *Systematic Biology* 67 (5): 901–904. <https://doi.org/10.1093/sysbio/syy032>
- RIMA – Relatório de Impacto Ambiental. 2004. *Projeto de Integração do Rio São Francisco com Bacias Hidrográficas do Nordeste Setentrional*. Ministério da Integração Nacional. Available from <https://antigo.mdr.gov.br/images/stories/ProjetoRioSaoFrancisco/ArquivosPDF/documentostecnicos/RIMAJULHO2004.pdf> [accessed 5 Oct. 2015].
- Roberto I.J. & Loebmann D. 2016. Composition, distribution patterns, and conservation priority areas for the herpetofauna of the state of Ceará, northeastern Brazil. *Salamandra* 52 (2): 134–152.
- Röhr D.L., Guimarães F.C.A., Martinez P.A., Mobley R.S.S., Juncá F.A. & Garda A.A. 2020. Habitat-dependent advertisement call variation in the monkey frog *Phyllomedusa nordestina*. *Ethology* 126 (6): 651–659. <https://doi.org/10.1111/eth.13017>
- Silva G.R., dos Santos C.L., Alves M.R., de Sousa S.D.V. & Annunziata B.B. 2010. Anfíbios das dunas litorâneas do extremo norte do Estado do Piauí, Brasil. *Sitientibus. Série Ciências Biológicas* 7 (4): 334–340.

- Silva F.P., Fernandes-Ferreira H., Montes M.A. & Silva L.G. 2020. Distribution modeling applied to deficient data species assessment: a case study with *Pithecopus nordestinus* (Anura, Phyllomedusidae). *Neotropical Biology and Conservation* 15: 165–175. <https://doi.org/10.3897/neotropical.15.e47426>
- Sueur J., Aubin T. & Simonis C. 2008. Seewave, a free modular tool for sound analysis and synthesis. *Bioacoustics* 18: 213–226. <https://doi.org/10.1080/09524622.2008.9753600>
- Toledo L.F. & Batista R.F. 2012. Integrative study of Brazilian anurans: relationship between geographic distribution, size, environment, taxonomy, and conservation. *Biotropica* 44 (6): 785–792. <https://doi.org/10.1111/j.1744-7429.2012.00866.x>
- Toledo L.F., Martins I.A., Bruschi D.P., Passos M.A., Alexandre C. & Haddad C.F.B. 2015. The anuran calling repertoire in the light of social context. *Acta Ethologica* 18 (2): 87–99. <https://doi.org/10.1007/s10211-014-0194-4>
- Valencia-Aguilar A., Ruano-Fajardo G., Lambertini C., Leite D.S., Toledo L.F. & Mott T. 2015. The chytrid fungus acts as a generalist pathogen that infects species-rich amphibian families in Brazilian rainforests. *Diseases of Aquatic Organisms* 114 (1): 61–67. <https://doi.org/10.3354/dao02845>
- Vilaça T., Silva J.R.S. & Solé M. 2011. Vocalization and territorial behaviour of *Phyllomedusa nordestina* Caramaschi, 2006 (Anura: Hylidae) from southern Bahia, Brazil. *Journal of Natural History* 45 (29–30): 1823–1834. <https://doi.org/10.1080/00222933.2011.561018>
- Watters J.L., Cummings S.T., Flanagan R.L. & Siler C.D. 2016. Review of morphometric measurements used in anuran species descriptions and recommendations for a standardized approach. *Zootaxa* 4072 (4): 477–495. <https://doi.org/10.11646/zootaxa.4072.4.6>
- Zhang J., Kapli P., Pavlidis P. & Stamatakis A. 2013. A general species delimitation method with applications to phylogenetic placements. *Bioinformatics* 29: 2869–2876. <https://doi.org/10.1093/bioinformatics/btt499>

Manuscript received: 11 April 2020

Manuscript accepted: 26 August 2020

Published on: 10 November 2020

Topic editor: Rudy Jocqué

Desk editor: Radka Rosenbaumová

Printed versions of all papers are also deposited in the libraries of the institutes that are members of the *EJT* consortium: Muséum national d'histoire naturelle, Paris, France; Meise Botanic Garden, Belgium; Royal Museum for Central Africa, Tervuren, Belgium; Royal Belgian Institute of Natural Sciences, Brussels, Belgium; Natural History Museum of Denmark, Copenhagen, Denmark; Naturalis Biodiversity Center, Leiden, the Netherlands; Museo Nacional de Ciencias Naturales-CSIC, Madrid, Spain; Real Jardín Botánico de Madrid CSIC, Spain; Zoological Research Museum Alexander Koenig, Bonn, Germany; National Museum, Prague, Czech Republic.

Appendix 1. Comparative material examined.

Pithecopus azureus

ARGENTINA • Corrientes MNRJ 39995.

BRAZIL – **Mato Grosso do Sul** • Bela Vista; AAG-UFU 0148 to 0153 • Bela Vista; MNRJ 61567 to 61571.

PARAGUAY • Asunción; MNRJ 13657 to 13662, 13664 to 13670.

Pithecopus hypochondrialis

BRAZIL – **Pará** • Prainha; ZUEC 16511, 16520, 16515, 16529, 16530 • Monte Alegre; ZUEC 19916, 19940, 19944, 19945 • Alenquer; ZUEC 19917, 19920, 19923, 19927, 19930, 19932 • Oriximiná; ZUEC 19918, 19922, 19926, 19928 • Óbidos; ZUEC 19921, 19933, 19938, 19943. – **Amapá** • Laranjal do Jari; ZUEC 16550, 16551, 16553, 16555, 16559, 16561, 16562, 16605 • Serra do Navio; AAG-UFU 5987 to 5989, 5998 to 6000. – **Mato Grosso** • Barra do Garças; ZUEC 21650 • Barra do Garças; AAG-UFU 3489 to 3494, 1078 to 1084. – **Goiás** • Guarani de Goiás; AAG-UFU 1963, 1964 • Uruaçu; AAG-UFU 0991 to 0993, 0996 to 0999 • Pirenópolis; AAG-UFU 0331, 0334 • Padre Bernardo; AAG-UFU 0117, 0118 • Chapada dos Veadeiros; AAG-UFU 1333 • Mineiro; AAG-UFU 3410. – **Tocantins** • Paranã; AAG-UFU 2827 to 2830 • Palmas; AAG-UFU 2779, 2817. – **Minas Gerais** • Uberlândia; AAG-UFU 2311, 2313, 2315, 2299, 3256 • Araguari; AAG-UFU 3101, 3116, 4573, 4689, 4936, 4937, 4832, 4834 • Ituiutaba; AAG-UFU 0455, 1276. – **Amazonas** • Manaus; ZUEC 16504 to 16509.

Pithecopus nordestinus

BRAZIL – **Bahia** • Alagoinhas; ZUEC 21661 to 21663, 21665 • Maracás; MNRJ 13598 to 13611, 35223 to 35228, 60097. – **Sergipe** • Areia Branca; ZUEC 19882 to 19885, 19887 to 19894, 19898, 19899, 19901, 19902, 19906, 19907, 19909, 19911 • Laranjeiras; ZUEC 19895, 19897, 19900, 19903, 19908, 19912, 19913.

Pithecopus rohdei

BRAZIL – **Rio de Janeiro** • Itaguaí; ZUEC 1223, 1224, 5229, 5230, 7716 • Seropédica; ZUEC 16130.

Pithecopus megacephalus

BRAZIL – **Minas Gerais** • Jaboticatubas; ZUEC 1651, 3004 to 3006, 3428, 15444.

Pithecopus ayeaye

BRAZIL – **Minas Gerais** • Poços de Caldas; AAG-UFU 1661 to 1664, 3523 to 3525 • Poços de Caldas; ZUEC 4160, 4161, 4289 to 4291, 4293, 4470, 4481, 6854 • Alpinópolis; AAG-UFU 0962 to 0964.

Pithecopus palliatus

BRAZIL – **Acre** • Cruzeiro do Sul; ZUEC 5388, 5392 • Xapuri; ZUEC 5685 to 5695, 5740, 5741, 5754, 5760.

Pithecopus rusticus

BRAZIL – **Santa Catarina** • Água Doce; UFMG 13360 to 13362, 13353 to 13359.

Supplementary material

Supplementary file 1. Analysed sound files (*.wav format) of the four species of *Pithecopus* Cope, 1866: *P. araguaeus* Haga *et al.*, 2017, *P. hypochondrialis* (Daudin, 1800), *P. azureus* (Cope, 1862), *P. nordestinus* (Caramaschi, 2006) and *P. gonzagai* sp. nov. <https://doi.org/10.5852/ejt.2020.723.1147.3071>

Supplementary file 2. Detailed specimens used for phylogenetic inferences. Genbank details, voucher numbers, sample locality. <https://doi.org/10.5852/ejt.2020.723.1147.3073>

Supplementary file 3. Raw morphometric measurement dataset (values in millimetres) of examined specimens of *Pithecopus* Cope, 1866, which were used for statistical analysis. <https://doi.org/10.5852/ejt.2020.723.1147.3075>

Supplementary file 4. Eigenvectors of the DAPC based on morphological traits. <https://doi.org/10.5852/ejt.2020.723.1147.3077>

Supplementary file 5. Eigenvectors of the DAPC based on acoustic traits. <https://doi.org/10.5852/ejt.2020.723.1147.3079>

Supplementary file 6. Phylogenetic relationships of the *Pithecopus* Cope, 1866 based on 16S rDNA mitochondrial fragment. Expanded topology inferred from the Bayesian inference based on the *GTR+G* model. *Pithecopus gonzagai* sp. nov. in blue and *P. nordestinus* (Caramaschi, 2006) in red. Posterior probabilities are shown at each node. Scale bar represents the number of substitutions per site. ID numbers corresponding to [Supplementary file 2](https://doi.org/10.5852/ejt.2020.723.1147.3081). <https://doi.org/10.5852/ejt.2020.723.1147.3081>

Supplementary file 7. Phylogenetic relationships of the *Pithecopus* Cope, 1866 based on NADH dehydrogenase subunit 2 (*ND2*) mitochondrial fragment. Expanded topology inferred from the Bayesian inference based on the *HKY+G+I* model. *Pithecopus gonzagai* sp. nov. in blue and *P. nordestinus* (Caramaschi, 2006) in red. Posterior probabilities are shown at each node. Scale bar represents the number of substitutions per site. ID numbers corresponding to [Supplementary file 2](https://doi.org/10.5852/ejt.2020.723.1147.3083). <https://doi.org/10.5852/ejt.2020.723.1147.3083>

Supplementary file 8. Phylogenetic relationships of the *Pithecopus* Cope, 1866 based on Seven in Absentia Homolog 1 (*Siah*) nuclear fragment. Expanded topology inferred from the Bayesian inference based on the K2P model. *Pithecopus gonzagai* sp. nov. in blue and *P. nordestinus* (Caramaschi, 2006) in red. Posterior probabilities are shown at each node. Scale bar represents the number of substitutions per site. ID numbers corresponding to [Supplementary file 2](https://doi.org/10.5852/ejt.2020.723.1147.3085). <https://doi.org/10.5852/ejt.2020.723.1147.3085>

Supplementary file 9. Phylogenetic relationships of the *Pithecopus* Cope, 1866 based on 16S + *ND2* + *Siah* markers. Expanded topology inferred from the Bayesian inference. *Pithecopus gonzagai* sp. nov. in blue and *P. nordestinus* (Caramaschi, 2006) in red. Posterior probabilities are shown at each node. Scale bar represents the number of substitutions per site. ID numbers corresponding to [Supplementary file 2](https://doi.org/10.5852/ejt.2020.723.1147.3087). <https://doi.org/10.5852/ejt.2020.723.1147.3087>